DESIGN AND ANALYSIS OF RECTANGULAR MICROSTRIP PATCH ANTENNAS LOADED WITH PLASTIC AND BARIUM TITANATE SUBSTRATES

A thesis submitted in partial fulfillment of the requirement for the degree of

Master of Science in Electrical and Electronic Engineering

by

Md. Ababil Hossain

STUDENT NUMBER: 0412062239 F

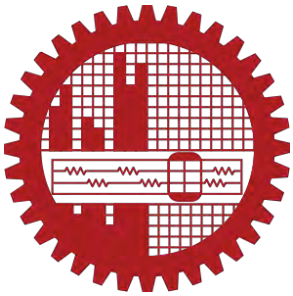

Department of Electrical and Electronic Engineering

Bangladesh University of Engineering and Technology

Dhaka-1000

August, 2015

Certification

The thesis titled **"DESIGN AND ANALYSIS OF RECTANGULAR MICROSTRIP PATCH ANTENNAS LOADED WITH PLASTIC AND BARIUM TITANATE SUBSTRATES"** submitted by Md. Ababil Hossain, Student No: 0412062239, Session: April, 2012, has been accepted as satisfactory in partial fulfillment of the requirement for the degree of MASTER OF SCIENCE IN ELECTRICAL AND ELECTRONIC ENGINEERING on August 1, 2015.

BOARD OF EXAMINERS

1. _____

Dr. Md. Shah Alam — Chairman (Supervisor)
Professor
Department of Electrical and Electronic Engineering,
Bangladesh University of Engineering and Technology,
Dhaka – 1000, Bangladesh.

2. _____

Dr. Taifur Ahmed Chowdhury — Member (Ex-officio)
Professor and Head
Department of Electrical and Electronic Engineering,
Bangladesh University of Engineering and Technology,
Dhaka – 1000, Bangladesh.

3. _____

Dr. Md. Farhad Hossain — Member
Associate Professor
Department of Electrical and Electronic Engineering,
Bangladesh University of Engineering and Technology,
Dhaka – 1000, Bangladesh.

4. _____

Gp Capt Dr. Md. Hossam-E-Haider — Member (External)
Senior Instructor
Department of Electrical, Electronic and Communication Engineering,
Military Institute of Science and Technology (MIST)
Mirpur Cantonment, Dhaka-1216, Bangladesh.

Declaration

It is hereby declared that this thesis or any part of it has not been submitted elsewhere for the award of any degree or diploma and that all sources are acknowledged.

Signature of the Candidate

_____

Md. Ababil Hossain

To my honorable teacher

late Matin sir

Acknowledgment

First of all, I would like to thank Almighty Allah for giving me the strength and patience to complete this thesis even after so many obstacles. I really faced a very hard time when my the then supervisor honorable professor Dr. Md. Abdul Matin died suddenly while I was performing the experiments of this research. Despite the limitations of laboratory facilities, it was only his will and motivation that propelled me to fabricate the antennas and conduct all the experiments in the laboratory. He had actually inculcated in me a never-ending motivation and zeal towards my research efforts since my undergraduate level and given me the moral support during my hard times. His contribution in my life can hardly be exaggerated in true sense of the term.

I would then like to express my sincere gratitude to my thesis supervisor, Dr. Md. Shah Alam, Professor, Department of Electrical and Electronic Engineering, BUET, for his generous help, encouragement and support to complete this thesis after the death of my earlier supervisor. Without his cordial assistance and motivation at that critical juncture, I would never have been able to improve and complete the whole thesis from there.

I would like to thank Mr. Mohammad Asif Zaman, Assistant Professor of EEE department of BUET for his relentless assistance during my research work. Without his support and guidance in the laboratory, it would have been almost impossible for me to conduct the experiments by myself. I would also like to express my gratitude to Dr. A. K. M. Abdul Hakim and Dr. Md. Abdul Matin of Glass and Ceramic Department of BUET for their support. I would also like to thank all the lab assistants of BUET who helped me in labs even during their busiest times, especially Mr. Emdad of Microwave Engineering Laboratory of BUET. I am also thankful to my friends- Hasib, Mobarak, Khalid, Imtiaz and Turjo for their help during this thesis work.

I am grateful to all my teachers of BUET. They gave the knowledge and directions that have helped me throughout my life. The knowledge I learnt from the classes in my B.Sc. and M.Sc. levels were essential for this thesis.

My thank goes to all the members of the thesis committee for taking the time to evaluate my work. I am also thankful to the current head of EEE department, Prof. Taifur Ahmed Chowdhury

and the past head, Prof. Pran Kahai Saha for their support. I would also like to acknowledge my gratitude to the ECE department of Utah State University, USA for providing me the facilities to modify and upgrade the whole thesis.

Last, but not the least, I would like to acknowledge gratefulness to my parents. Whatever I have achieved in my life would never have been feasible without their relentless effort since my childhood.

Abstract

Patch antennas are a type of low profile antennas those can yield a nice broadside radiation pattern with a moderate gain. In patch antenna fabrication process, substrate selection is also very important since gain is much affected by the proper choice of substrate. In this research, experimental investigation with the fabricated antennas at two widely used GSM bands (900 MHz and 1800 MHz) have been done. Later the experimental results have been verified by simulations. Although in literature there are numerous examples of fabricated patch antennas, the novelty of this research is the way antennas have been fabricated based on its mathematical modeling. At the beginning, a 900 MHz rectangular patch antenna loaded with plastic substrate was fabricated and tested in the laboratory. This antenna showed some deviations in radiation characteristics. So, another rectangular patch antenna at 1800 MHz frequency loaded with the same substrate was fabricated. The experimental results of this antenna showed good resonance and radiation behavior. However, both the antennas constructed with plastic substrates became bulky and heavy. That is why, in order to reduce the size and weight of the antenna, a high permittivity material (barium titanate) was used as the substrate for 1800 MHz rectangular patch antenna. Since barium titanate substrate is available in powdered form for industrial use, suitable shaped substrate was fabricated in laboratory for using it in patch antenna. The gain and radiation characteristics of this antenna were satisfactory despite of the fact that the gain decreased by a certain amount due to using high permittivity material as the antenna substrate. The antennas were later simulated in HFSS (High Frequency Structural Simulator) software to verify the experimental results by keeping all the dimensions same as fabricated antennas. The experimental and simulation results of all the antennas showed good conformity except for the 900 MHz plastic loaded rectangular patch antenna, the radiation pattern of which showed comparatively higher deviation. It was not possible to investigate several other important characteristics of the antenna, such as- s-parameter, polarization ratio etc. due to limitation of lab equipments. For this reason, some other analogous characteristics (e.g. receveived power level instead of s-parameter) have been used. After reviewing all the experimental and simulation results, it can be concluded that all the fabricated antennas show moderate resonance and radiation characteristics which is comparable to their ideal cases.

TABLE OF CONTENTS

LIST OF TABLES

LIST OF FIGURES

Chapter 1

Introduction

1.1 Preface

An antenna is defined by Webster's Dictionary as "usually a metallic device (as a rod or wire) for radiating or receiving radio waves." The IEEE Standard Definitions of Terms for Antennas (IEEE Std 145-1983) defines the antenna or aerial as a mean for radiating or receiving radio waves. In other words, the antenna is the transitional structure between free space and a guiding device. The guiding device or transmission line may take the form of a coaxial line or a hollow pipe waveguide; and it is used to transport electromagnetic energy from the transmitting source to the antenna or from the antenna to the receiver. In the former case, we have a transmitting antenna and in the latter, a receiving antenna [1].

Antennas are key components of wireless communication systems. An antenna transfers an electrical signal to electromagnetic waves that propagate through space and can be received by another antenna. It is usually used with a radio transmitter or radio receiver. In transmission, a radio transmitter supplies an electric current oscillating at radio frequency i.e., a high frequency alternating current (AC)) to the antenna's terminals, and the antenna radiates the energy from the current as electromagnetic waves (radio waves). In reception, an antenna intercepts some of the power of an electromagnetic wave in order to produce a tiny voltage at its terminals, that is applied to a receiver to be amplified.

Antennas can be of different types, such as- wire antennas, reflector antennas, aperture antennas, microstrip antennas etc. Different types of antennas are used for different purposes. As for example- highly directive antennas are required for satellite communications, whereas omnidirectional antennas are preferable in mobile

communication. Nowadays, low profile antennas are required especially in high performance aircraft, spacecraft, and satellite and missile applications [1]. In order to meet their requirements, microstrip patch antennas provide significant advantages such as low profile, low weight, relatively low manufacturing cost and polarization diversity [2-5]. Metamaterial based patch antennas may be good solutions to meet all these requirements [6, 7]. But due to the fabrication complexity of metamaterials at laboratory, it may be convenient to use conventionally available dielectrics, such as- plastic, teflon etc. or artificially fabricated dielectric materials such as- barium titanate as the substrates of patch antenna for obtaining appreciable performance at the desired frequency.

Patch Antennas can be of different shapes such as- rectangular, circular, elliptical etc. Due to simpler geometric structure, rectangular patch antennas are preferable in many applications. Radiation performance of rectangular patch antennas is also comparatively better [8]. In literature, there are several descriptions of practical construction of patch antennas of different shapes loaded with conventional and unconventional dielectrics [9-13]. However, the bandwidth, gain, return loss, radiation efficiency etc. of these antennas may vary due to the use of different dielectrics as substrate. So, for optimum antenna performance at the desired frequency, proper choice of the substrate is also very important.

1.2 Literature Review

Over the last few decades, researchers over the world have proposed the design methods of different types of patch antennas. Many of them also practically fabricated and tested those antennas in the laboratory. In [10], Islam *et. al* designed and fabricated a coaxially-fed single-layer compact microstrip patch antenna for achieving dual-polarized radiation suitable for applications in the IEEE Radar Band, C and X. The designed antenna consists of three rectangular patches which overlapped along their diagonals shown in Fig. 1.1.

(a) (b)

Fig. 1.1: Fabricated antenna by Islam *et al.*[10] a) top view
b) back view.

The basic configuration of the proposed patch antenna for exciting dual-band dual-polarization is illustrated in Fig. 1.2. The dimensions of the patches are (13× 9) mm^2. S_1 and S_2 indicate the overlapping dimensions of the patches which are 4.5 mm and 6.5 mm. A dielectric substrate of relative permittivity ε_r= 2.2 and thickness of h = 1.58 mm are chosen. The radiating patch is fed by a coaxial probe type feed in this design. The feed location at f_p = 4.43 mm is used. The structure has three different resonant lengths as follows-

$$l_1 = W + (W - S_2) + 2\Delta l_1$$
$$l_2 = L + (L - S_1) + 2\Delta l_2$$
$$l_3 = W + L - (L - S_1) + 2\Delta l_3$$

Where Δl_1, Δl_2 and Δl_3 are the increase in resonant lengths due to fringing fields at three different frequencies

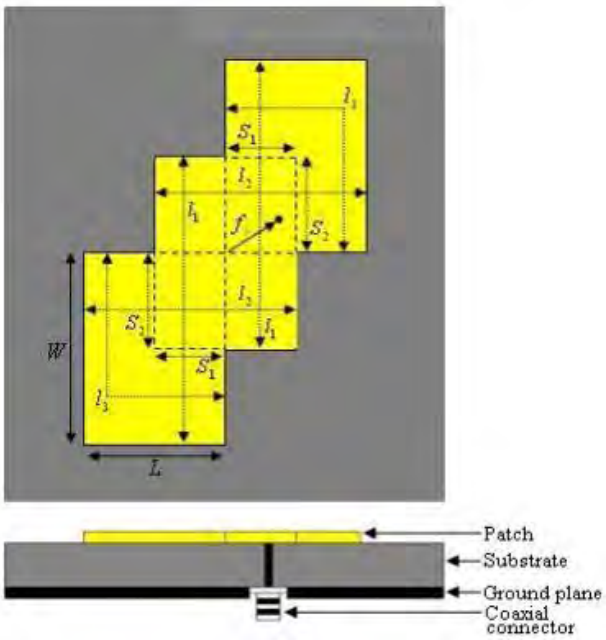

Fig. 1.2: Schematics of the probe feed microstrip patch antenna (upper portion indicates top view, and lower portion indicates side view).

The designed antenna showed good resonant results. It showed a bandwidth of 154 MHz at f_0=6.83 GHz and 209 MHz at f_0=9.73GHz as depicted in Fig. 1.3.

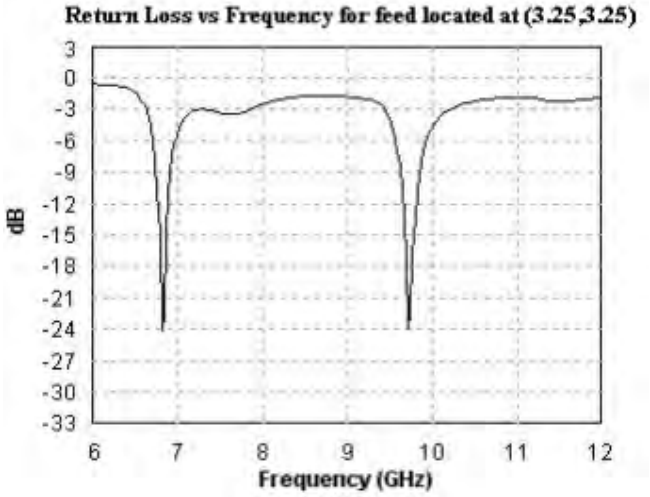

Fig. 1.3: Return loss of fabricated antenna in [10] for feed located at the position (3.25mm, 3.25mm) in XY plane.

In [11], Bordoloi *et al.* fabricated and tested a tunable rectangular patch antenna, designed to resonate at 3.25 GHz using adjustable air pocket in the substrate layer with a sliding arm. The dielectric material selected for the antenna was FR4 which has a dielectric constant of 4.8 and height of dielectric substrate was kept 3 mm. Overall dimension of the patch was 26 mm x 23 mm and the antenna was fed by a 50 ohm microstrip line as shown in Fig. 1.4.

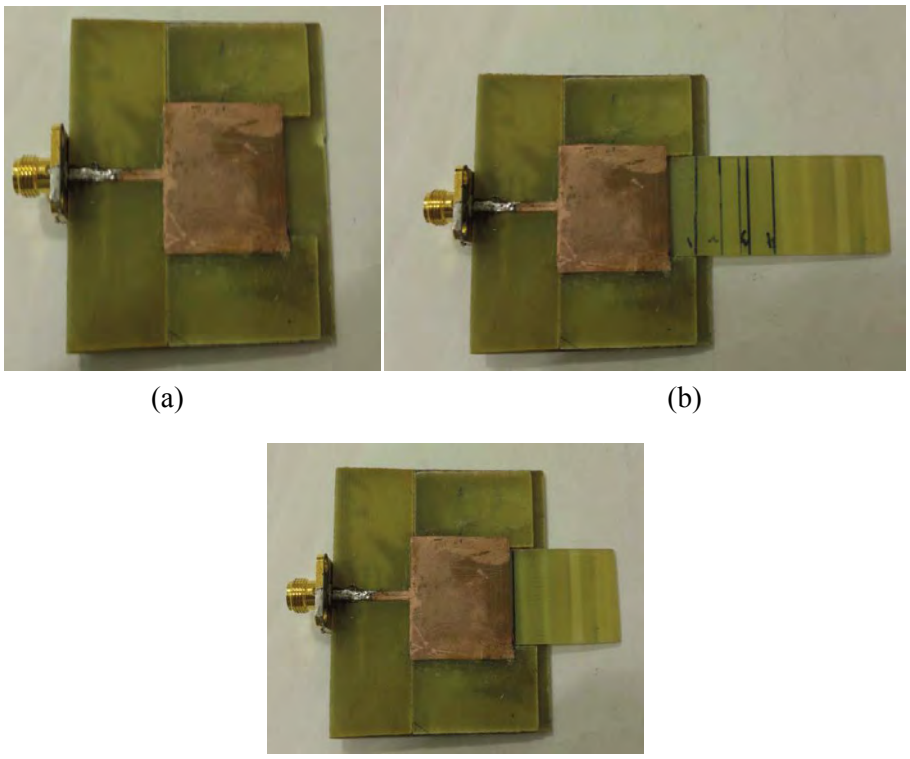

(a) (b)

(c)

Fig. 1.4: (a) The structure of the Bordoloi *et. al's* [11] patch antenna with dielectric portions cut away; (b) and (c) Patch Antenna with sliding arm at two positions.

A dielectric section below the patch is milled away and an air pocket layer is being formed as shown in figure above. The sliding arm, consisting of the same dielectric material is inserted inwards for tuning purpose. So, the resonant frequency of the patch changes as the effective dielectric constant varies for different dielectric gap- lengths in

substrate layer. The return loss (s-parameter) of the antenna was measured frequency which showed nearly -10 dB for almost all types of tuning shown in Fig. 1.5.

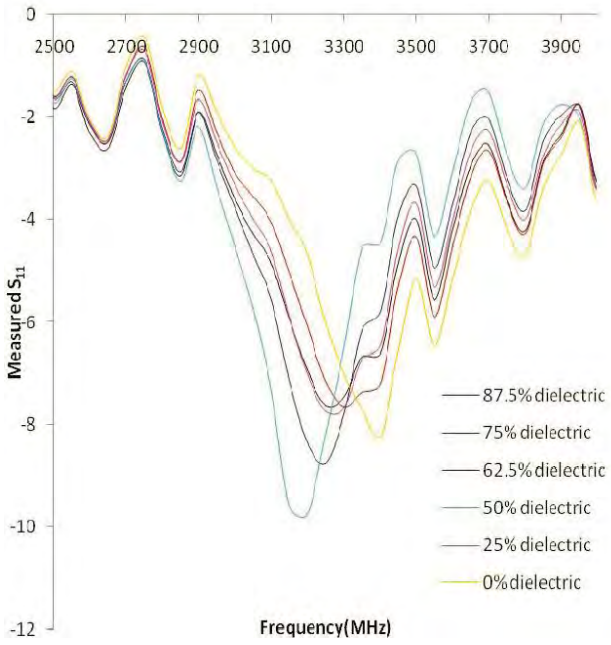

Fig. 1.5: Measured S_{11} versus frequency at different positions of the sliding arm.

From Fig 1.5, it is evident that as the percentage of dielectric increases in the gap, the resonant frequency shifts towards left due to the increase of effective dielectric constant. When the air pocket below the patch is 50%, best matching is observed with the return loss nearly equal to -10dB. A maximum frequency shift towards left side is observed when the dielectric is 50% filled in the air pocket. Frequency shift reduces with further increase in the air pocket. However, with increase in air gap, the resonant frequency shifts towards the higher side. In this process, by changing the position of the sliding arm, frequency shift of up to 150 MHz was obtained by Bordoloi *et al.'s* antenna.

Wong *et al.* designed and fabricated a dual band slotted circular patch antenna where the modification of TM_{210} Mode was done with symmetrical slotting. Design of a circular patch single feed dual-frequency circular microstrip antenna with a pair of arc-shaped slots [14], a single arc-shaped slot [15] and an open-ring slot [16] have previously been reported by Wong. The case with a pair of arc-shaped slots is discussed below:

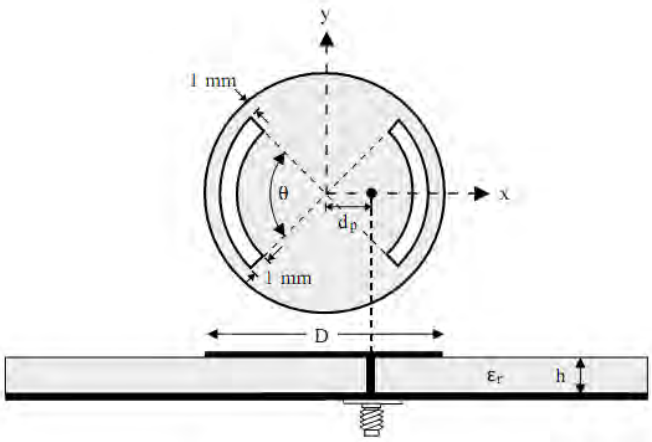

Fig. 1.6: Geometry of a dual-frequency circular microstrip antenna with a pair of arc-shaped slots (Wong *et al.'s* fabricated antenna [14]).

In the geometry shown in Fig 1.6, two arc-shaped slots, having a narrow width of 1 mm and subtended by an angle θ, are placed close to the boundary of the circular patch at a distance of 1 mm. The two arc-shaped slots are centered with respect to the x axis. A single probe feed for dual-frequency operation is placed along the x axis at a distance d_p from the patch center. With the presence of the slots, the fundamental mode TM_{110} of the circular microstrip antenna is slightly perturbed because the slots are located close to the patch boundary, where the excited patch surface current for the TM_{110} mode has a minimum value; that is, the resonant frequency f_{110} will be slightly varied by the introduced slots in the circular patch.

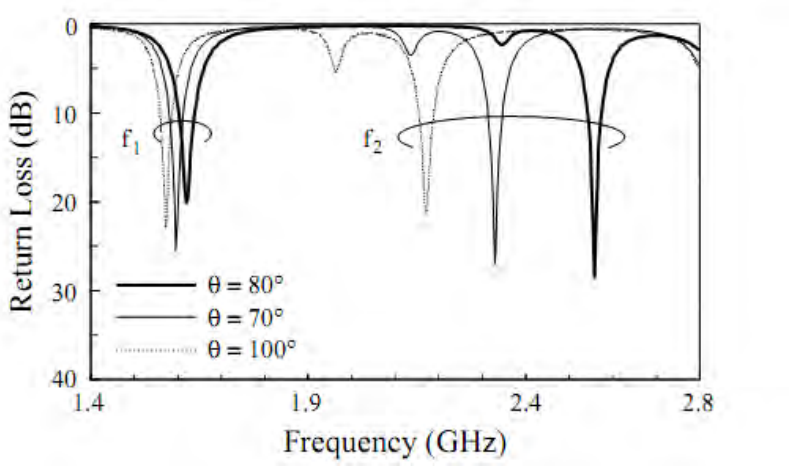

Fig. 1.7: Measured return loss for the antenna in [14]; ε_r= 4.4, h =1.6 mm, and D = 50 mm.

The second resonant mode excited in the design is the TM_{210} mode. Since the excited patch surface current for the TM_{210} mode is very close to the patch boundary, it is expected that the TM_{210} mode will be significantly perturbed due to the presence of the slots. From the simulated results using IE3DTM, it was found by Wong *et al.* that the patch surface current path of the TM_{210} mode was lengthened and strongly modified such that the excited patch surface currents circulate around the two arc-shaped slots, and a resonant condition with nulls close to the edges of the two slots is obtained. This suggests that the resonant frequency f_{210} will be significantly decreased, and the current distribution of the perturbed TM_{210} mode will become similar to that of the TM_{110} mode; that is, the radiation pattern of the perturbed TM_{210} mode will become similar to that of the TM_{110} mode. Thus, from the results obtained, it is expected that dual-frequency operation of the same polarization planes and similar radiation characteristics for the present antenna can be obtained. Experiments have been conducted on this design. Fig. 1.7 shows the measured return loss for the cases with θ = 80◦, 90◦ and 100◦. The diameter of the circular patch is selected to be 50 mm and the microwave substrate used has a

thickness h = 1.6 mm and a relative permittivity of $\varepsilon_r = 4.4$. The resonant frequencies f_{110} and f_{210} of the present design without slots are 1.65 and 4.77 GHz, respectively.

It is seen that the first resonant frequency, f_1 is about 1.6 GHz, very slightly affected by the variation in the subtending angle of various arc-shaped slots. On the other hand, the second resonant frequency f_2 is significantly decreased with increasing θ, and is much lower than the resonant frequency of the unperturbed TM_{210} mode of the case without slots. The feed positions are insensitive to various arc-shaped slots introduced in the present design and fixed at d_p =12 mm from the patch center. The frequency ratio f_2/ f_1 of the two operating frequencies is within the range of 1.38–1.58. These two operating frequencies have the same polarization planes and similar radiation patterns. Good cross-polarization radiation is observed for the two operating frequencies.

In [9], Jahani *et al.* proposed light, low-cost, and easy-to-fabricate circular patch antennas loaded by helices operating as MNG metamaterials in order to miniaturize patch antennas without using any dielectric in the antenna substrate [9]. It has been shown theoretically that the sub-wavelength radiating mode of a circular patch antenna may exist if a homogeneous and isotropic MNG core is surrounded by a conventional material. The sub wavelength radiation frequency depends on the ratio of the core radius to the patch radius and also the ratio of MNG metamaterial permeability to the surrounding dielectric permeability. Since the patch operates at sub wavelength frequencies, dimensions of the unit cell must be of the order of or less. Helices can operate as MNG core in the antenna substrate. They are small in size, and their manufacturing, testing, and loading to the air substrate are more convenient than other MNG metamaterials, such as split-ring resonators (SRRs) and SRs. Volumes containing helices exhibit Lorentzian form for permeability.

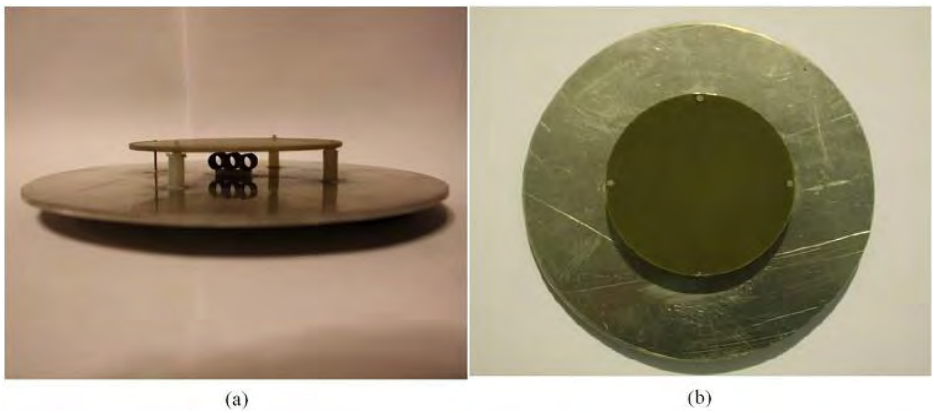

Fig. 1.8: Miniaturized patch antenna loaded with helical metamaterials (Jahani *et al.'s* antenna [9]) (a) Side view (b) Top view.

Fig. 1.8 shows Jahani *et al.*'s patch antenna configuration. Three helices are located at the center of the patch where the maximum amplitude of the magnetic field is predicted theoretically. The axes of helices are parallel to the magnetic field vector to support the MNG behavior. The radius of the patch and ground are 42 and 80 mm, respectively; the thickness of substrate is selected to be 12 mm such that the helices can be easily located underneath the patch. Three thin teflon cylinders and a small stand underneath the helices are used to keep the patch and helices within the air substrate. The antenna is fed by a coaxial probe fixed to the aluminum ground plane and placed close to the patch edge. The antenna is light, and it has an approximate total weight of 160 g. The resonant frequency of the patch depends on the metamaterial permeability. By increasing the number of turns or the radius or by decreasing the spacing between adjacent turns of each helix, metamaterial resonant frequency decreases. To investigate the relationship of antenna performance and size reduction, Wong fabricated two antennas with different metamaterial parameters. For the first case, helices with nine turns are selected from a copper wire with a diameter of 0.7 mm whose spacing between adjacent turns and whose radius are 0.6 and 3 mm respectively. For the second one, numbers of turns are five, wire

diameter is 0.4 mm, spacing between adjacent turns is 1 mm, and the radius of helices is 3 mm.

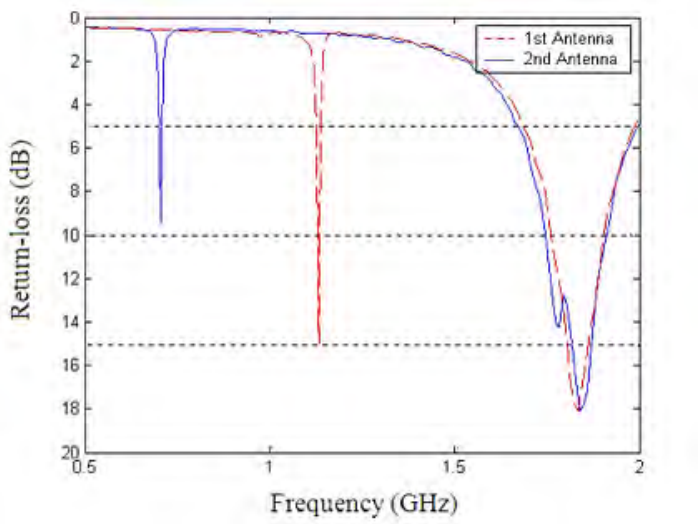

Fig. 1.9: Measured return loss for fabricated antennas of Jahani *et al.*[9].

Fig. 1. 9 shows the measured results of return loss for the proposed antennas using the HP8510C vector network analyzer. Since metamaterials behave as regular dielectrics at frequencies far from their resonant frequencies, the higher patch resonance (1.85 GHz for both antennas) equals the conventional resonance of a patch antenna. The lower one (1.126 GHz for the first antenna and 0.703 GHz for the second) however corresponds to the sub wavelength resonance. These frequencies are close to the calculated resonant frequencies of helices. Size reduction is about 40% for the first and 60% for the second. The bandwidth decreases at sub wavelength resonances because of narrowband nature of these types of metamaterials. For the first design, -10 dB return loss bandwidth is about 0.5% at lower resonance.

The radiation patterns of the antennas were measured in a shielded pyramidal anechoic chamber using three-antenna technique with two standard-gain horn antennas. The measured results shows good radiation characteristics both at sub wavelength resonances and at primary mode as depicted in Fig. 1.10.

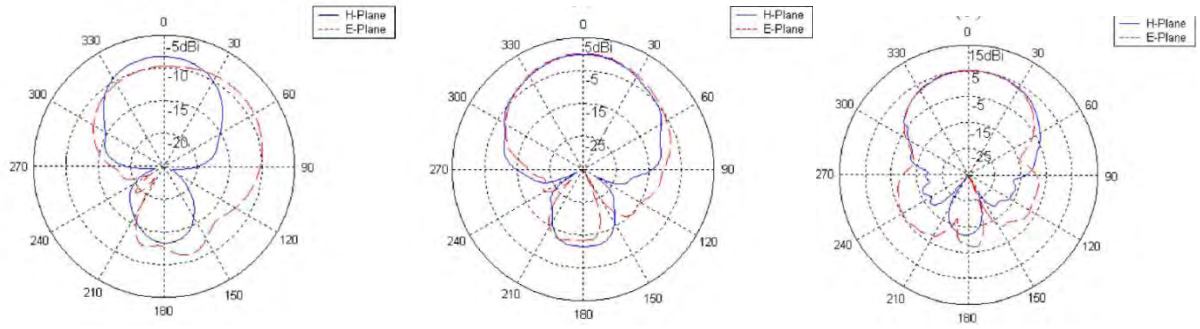

(a) (b) (c)

Fig. 1.10: Measured radiation pattern in [9] for (a) the second antenna at 0.703 GHz, (b) the first antenna at 1.126 GHz, and (c) both antennas at 1.85 GHz.

1.3 Objectives of the Thesis

The objective of this thesis is to analyze the performance of practically fabricated rectangular patch antennas designed at GSM band frequencies of 900 MHz and 1800 MHz, and then compare the results with their simulations. The following steps will be followed for the design and practical implementation purpose of the antennas:

i. First, the permittivity of two different types of antenna substrates (plastic and barium titanate) will be measured by an impedance analyzer. Then based on this result, the length, width and other parameters of the patch and ground plane of the will be fixed accordingly.

ii. Later, the radiation performance of the fabricated rectangular patch antennas with calculated length, width and other parameters will be observed at the desired GSM 900 MHz and 1800 MHz frequencies.

iii. The expected result will be the change in patch sizes at the desired frequency due to using different types of substrates for the patch antennas. At first, a larger sized patch antenna loaded with plastic substrate, operating at 900 MHz

frequency will be constructed and tested in the laboratory. Then same will be done for a smaller sized antenna of 1800 MHz, loaded with both plastic and barium titanate substrates.

iv. Simulation results will be analyzed to verify the experimental results of the patch antennas.

1.4 Organization of the Thesis

The thesis consists of six chapters. The chapters cover the theory, design procedure, experimental investigation and numeric results.

Chapter 1 contains preface, a brief literature review of previous works on fabricated patch antennas and organization details of the whole thesis.

Chapter 2 contains theoretical background of antennas which includes some fundamentals of general antennas and then a section on patch antenna theory.

Chapter 3 is on practical construction procedure of the proposed antennas. It includes substrate analysis, laboratory fabrication of barium titanate substrate and measurement process of permittivity of substrates through impedance analyzer. Later, it provides the description of the fabricated patch antennas at GSM 900 and 1800 MHz frequency bands loaded with both plastic and barium titanate substrates.

Chapter 4 contains experimental investigation with the fabricated patch antennas in the laboratory. Initially a description of the experimental set-up in the laboratory has been given. Later, it shows radiation pattern investigation of all three patch antennas loaded with plastic and barium titanate substrates.

Chapter 5 presents simulation results of the patch antennas and comparison of experimental and simulated antenna results.

Chapter 6 contains a summary and future scope of the work. It concludes with a discussion on what can be done to improve the fabricated antenna design and performance, thus paving the way for the idea of more sophisticated antennas.

Chapter 2

Theoretical Background

During 1890s, there were only a few antennas in the world. These rudimentary devices were primarily a part of experiments that demonstrated the transmission of electromagnetic waves. By World War II, antennas became so ubiquitous that their use had transformed the lives of the average person via radio and television reception. The number of antennas in the United States was on the order of one per household during the same period. However, by the early 21st century, the average person in US now carries one or more antennas on them wherever they go, in the form of cell phones and other electronic devices. So, people involved in antennas and wireless communication network should possess sufficient knowledge in antenna engineering. Antenna fundamentals are discussed in this chapter. In order to investigate the radiating properties and mechanism of antenna radiation, theoretical knowledge on antenna and its different fundamental parameters is a must. In the first part of this chapter, definition of general antenna parameters are given with illustration. In the later part, patch antenna theory has been discussed.

2.1 Fundamental Topics of Antenna

2.1.1 Introduction

The first antennas were built in 1886 by German physicist Heinrich Hertz in his pioneering experiments to prove the existence of electromagnetic waves predicted by the theory of James Clerk Maxwell [17]. Hertz placed dipole antennas at the focal point of parabolic reflectors for both transmitting and receiving. He later published his work

in *Annalen der Physik und Chemie*. Since then many theoretical modeling on much more sophisticated antennas, and practical researches on many of those have been carried out in the last century.

2.1.2 Types of Antennas

There are many fundamental antenna types. Different types of antennas are necessary for different purposes. Some specific applications such as- satellites require highly directive antennas, while some others need omni-directional antennas, such as- cell phones. On the basis of shapes and performance, antenna can be classified as follows-

i) Wire Antennas
ii) Aperture Antennas
iii) Microstrip Antennas
iv) Array Antennas
v) Reflector Antennas
vi) Lens Antennas

Wire Antennas:

Wire Antennas are familiar to the layman because they are virtually seen on everywhere- on automobiles, buildings, ships, spacecrafts, aircrafts and so on [1]. There are various shapes of wire antennas, such as a straight wire (dipole), loop and helix. Loop antennas need not only be circular. They may take the form of a rectangle, square, ellipse, or any other configuration. The circular loop is the most common because of its simplicity in construction.

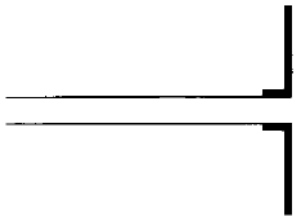

(a) Dipole antenna

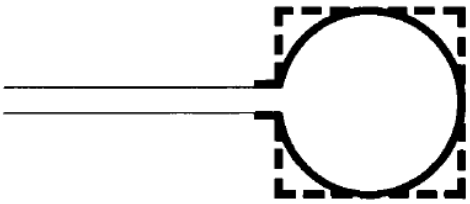

(b) Circular loop antenna

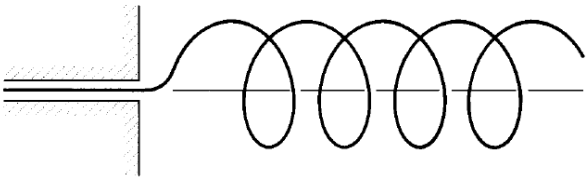

(c) Helix antenna

Fig. 2.1: Different types of wire antennas [1].

Aperture Antennas:

Because of increasing demand for more sophisticated forms of antennas and utilization of higher frequencies, aperture antennas have become more familiar today [1]. Some forms of aperture antennas are shown in Fig. 2.2. Antennas of this type are very useful for aircraft and spacecraft applications, because they can be very conveniently flush-mounted on the skin of the aircraft or spacecraft [1]. In addition, they can be covered with a dielectric material to protect them from hazardous conditions of the environment.

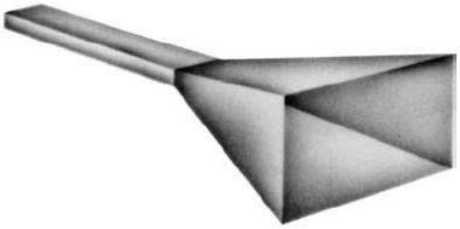

(a) Pyramidal horn antenna

(b) Conical horn antenna

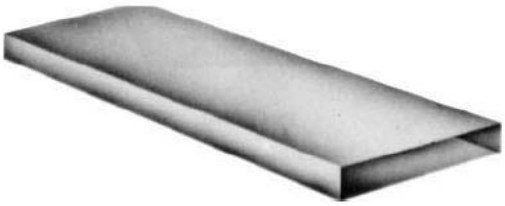

(c) Rectangular waveguide

Fig. 2.2: Different types of aperture antennas [1].

Microstrip Antennas:

Microstrip antennas became popular in the 1970s primarily for the space borne applications [1]. Today they are used for government and commercial applications. Theses antennas consists of a metallic patch on a grounded substrate. The metallic patch can take many different configurations . However the rectangular and circular patches are the most popular because of ease of analysis and fabrication, and their attractive radiation characteristics, especially low cross-polarization radiation. The microstrip antennas are low-profile, comfortable to planar and non-planar surfaces, simple and inexpensive to fabricate using modern printed circuit technology, mechanically robust when mounted on rigid surfaces, compatible with MMIC designs, and very versatile in terms of resonant frequency, polarization pattern, and impedance. These antennas can be mounted on the surface of high performance aircraft, spacecraft, satellites, missiles, cars and even handheld mobile telephones.

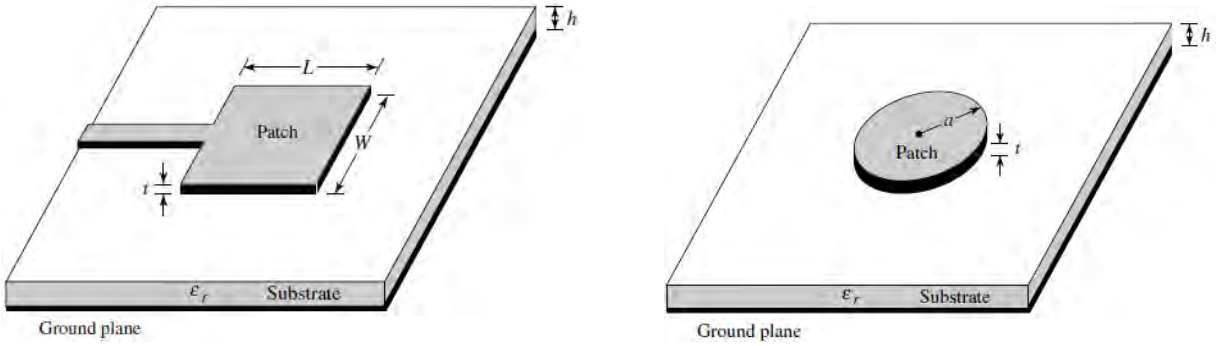

(a) Rectangular microstrip patch antenna

(b) Circular microstrip patch antenna

Fig. 2.3: Microstrip antennas of different shapes [1].

Array Antennas:

Many applications require radiation characteristics that may not be achievable by a single element. It may however be possible that an aggregate of radiating elements in an electrical and geometrical arrangements will result in the desired radiation characteristics. The arrangement of the array may be such that the radiation from the elements adds up to give a radiation maximum in a particular direction, minima in other directions.

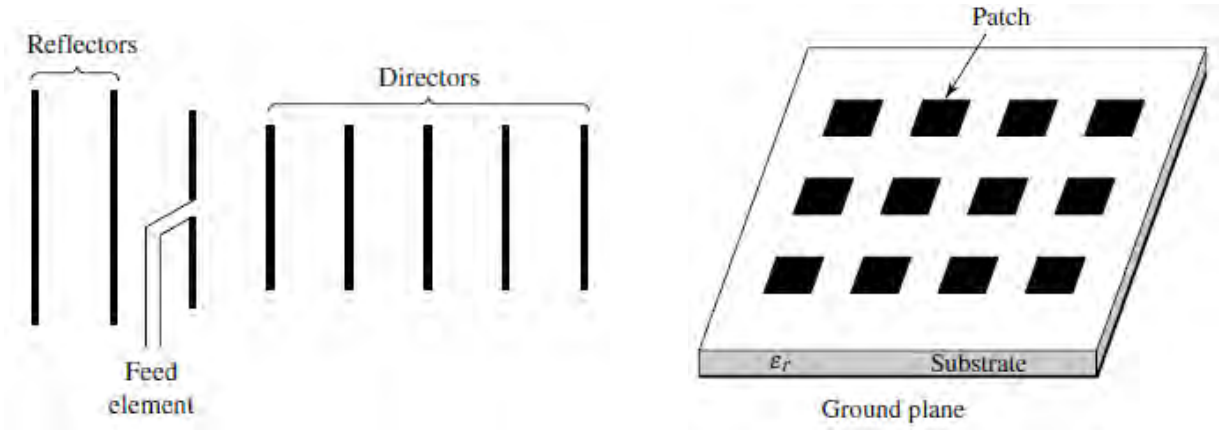

(a) Yagi uda array (b) Microstrip patch array

Fig. 2.4: Typical array configurations [1].

Reflector Antennas:

The success in the exploration of outer space has resulted in the advancement of antenna theory. Because of the need to communicate over great distances, sophisticated forms of antennas need to be used in order to transmit and receive signals that travel millions of miles. A very common antenna form for such an application is a parabolic reflector shown in Fig. 2.5(a). Antennas of this type have been built with diameters as large as 305 meters. Such large dimensions are needed to achieve the high gain required to transmit or receive signals after millions of miles of travel. Another form of a reflector, although not as common as the parabolic is the corner reflector as shown Fig. 2.5(b).

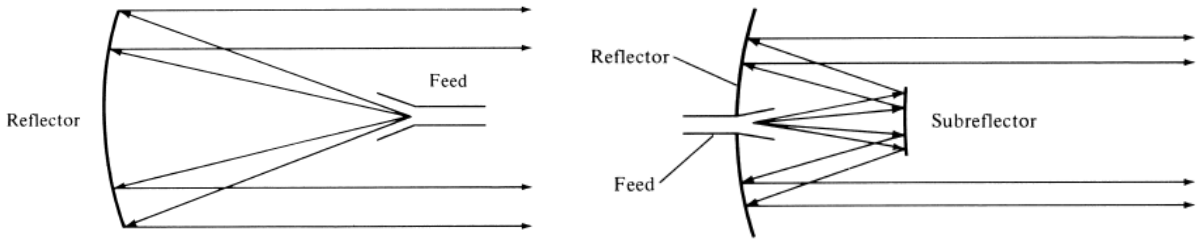

(a) Parabolic reflector with front Feed

(b) Corner reflector

Fig. 2.5: Typical reflector antenna configurations [1].

Lens Antennas:

Lenses are primarily used to collimate incident divergent energy to prevent it from spreading in undesired directions. By properly shaping the geometrical configuration and choosing the appropriate material of the lenses, they can transform various forms of divergent energy into plane waves [1]. They can be used in most of the same applications as are the parabolic reflectors, especially at higher frequencies. Their dimension and weight become exceedingly large at lower frequencies. Lens antennas are classified according to the materials from which they are constructed, or according to their geometrical shapes.

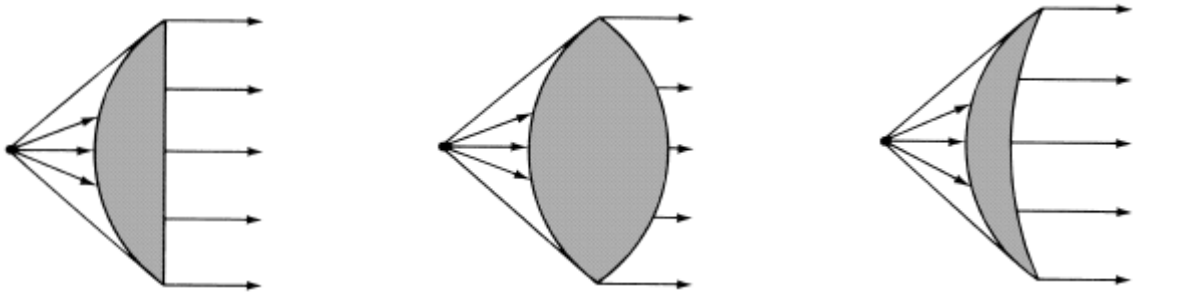

(a) Convex plane

(b) Convex-convex

(c) Convex-concave

Fig. 2.6: Different types of lens antenna configurations with index of refraction greater than 1 [1].

2.1.3 S-parameter (Return Loss)

S-parameter describes the input-output relationship between ports (or terminals) in an electrical system. For instance, if we have 2 ports (intelligently called Port 1 and Port 2), then S_{12} represents the power transferred from Port 2 to Port 1. S_{21} represents the power transferred from Port 1 to Port 2. S_{11} on the port of any radiator indicates the logarithmic value of the ratio between reflected and incident voltages. It is usually measured in dB. The smaller the value of S_{11}, lesser will be the power reflected back to the antenna. Mathematically it can be written by Eq. (2.1) [1].

$$S_{11}(dB) = 10\log(\frac{V_-}{V_+}) \qquad (2.1)$$

where,

V_- = Reflected Voltage

V_+ = Incident Voltage

For an antenna to operate properly, the value of S_{11} parameter should lie below -10 dB.

2.1.4 Radiation Pattern

A radiation pattern defines the variation of the power radiated by an antenna as a function of the direction away from the antenna. This power variation as a function of the arrival angle is observed in the antenna's far field. As an example, 3-dimensional radiation pattern for a dipole antenna is shown in Fig. 2.7.

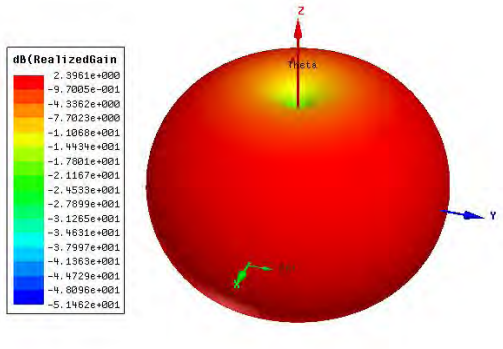

Fig. 2.7: 3D radiation pattern of a dipole antenna [37].

The above is an example of a donut shaped or toroidal radiation pattern. In this case, along the z-axis, which would correspond to the radiation directly overhead the antenna, there is very little power transmitted. In the x-y plane (perpendicular to the z-axis), the radiation is maximum. These plots are useful for visualizing which directions the antenna radiates.

2.1.5 Directivity

Directivity is a fundamental antenna parameter. It is a measure of how 'directional' an antenna's radiation pattern is. An antenna that radiates equally in all directions would have effectively zero directionality, and the directivity of this type of antenna would be 1 (or 0 dB). Mathematically, the formula for directivity (D) is written as in Eq. (2.2) [1].

$$D = \frac{1}{4\pi \int_0^{2\pi} 1. \int_0^{\pi} \left|F(\theta,\phi)\right|^2 \sin\theta d\theta d\phi} \tag{2.2}$$

This equation is a measure of the peak value of radiated power divided by the average, which gives the directivity of the antenna.

2.1.6 Gain

The term 'Gain' of an antenna describes how much power is transmitted in the direction of peak radiation to that of an isotropic source. An antenna with a gain of 3 dB means that the power received far from the antenna will be 3 dB higher (twice as much) than what would be received from a lossless isotropic antenna with the same input power. If D is the directivity and G is the gain of an antenna, then gain and directivity are related by Eq. (2.3) [1].

$$G = \eta D \tag{2.3}$$

where, η is the radiation efficiency of the antenna.

The gain of a real antenna can be as high as 40-50 dB for very large dish antennas (although this is rare). Directivity can be as low as 1.76 dB for a real antenna (example: short dipole antenna), but can never theoretically be less than 0 dB.

2.1.7 Antenna Efficiency

The efficiency of an antenna relates the power delivered to the antenna and the power radiated or dissipated within the antenna. A high efficiency antenna has most of the power present at the antenna's input radiated away. A low efficiency antenna has most of the power absorbed as losses within the antenna, or reflected away due to impedance mismatch. The losses associated within an antenna are typically the conduction losses (due to finite conductivity of the antenna) and dielectric losses (due to conduction within a dielectric which may be present within an antenna).

The antenna efficiency (or radiation efficiency) can be written as the ratio of the radiated power to the input power of the antenna in Eq. (2.4) [1].

$$\eta = \frac{P_{radiated}}{P_{input}} \tag{2.4}$$

Efficiency is ultimately a ratio, giving a number between 0 and 1. Efficiency is very often quoted in terms of a percentage; for example, an efficiency of 0.5 is the same as 50%.

2.1.8 Bandwidth

Bandwidth is another fundamental antenna parameter. Bandwidth describes the range of frequencies over which the antenna can properly radiate or receive energy. Often, the desired bandwidth is one of the determining parameters used to decide upon an antenna. For instance, many antenna types have very narrow bandwidths and cannot be used for wideband operation. In Table-2.1, bandwidth ranges for different antennas are shown.

Table-2.1: The bandwidth for several common antennas [18]

Antenna Type	Centre Frequency	Frequency Range	Frantional Bandwidth	Ratio	Percentage bandwidth
Patch	1000 MHz	985-1015 MHz	0.03	1.0305:1	3%
Dipole	1000 MHz	960-1040 MHz	0.08	1.083:1	8%
Horn	1000 MHz	154-1848 MHz	1.694	12:1	169.40%
Spiral	1000 MHz	95-1900 MHz	1.805	20:1	180.50%

2.1.9 Polarization

An antenna is a transducer that converts radio frequency electric current to electromagnetic waves that are then radiated into space. The electric field plane determines the polarization or orientation of the radio wave. In general, most antennas radiate either linear or circularly polarized manner. A linearly polarized antenna radiates wholly in one plane containing the direction of propagation, whereas in a circularly polarized antenna, the plane of polarization rotates in a circle making one complete revolution during one period of the wave. If the rotation is clockwise looking in the direction of propagation, the sense is called right-hand-circular (RHC). If the rotation is counter clockwise, then it is called left-hand-circular (LHC).

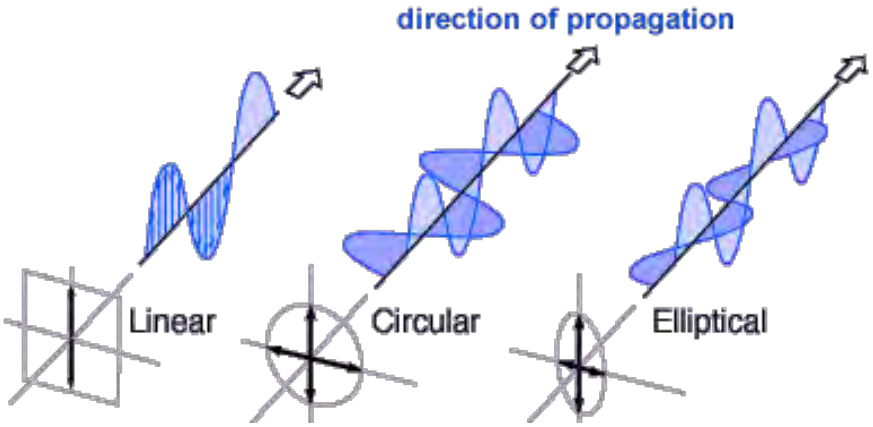

Fig. 2.8: Different types of polarization [19].

2.2 Patch Antenna Theory

2.2.1 Introduction

Microstrip or patch antennas are becoming increasingly useful because they can be printed directly onto a circuit board. These antennas are becoming very widespread within the mobile phone market. Patch antennas are low cost, have a low profile and are easily fabricated. However, some major operational disadvantages are their low efficiency, high Q (sometimes in excess of 100), poor polarization purity, poor scan performance, spurious feed radiation and very narrow frequency bandwidth, which is typically only a fraction of a percent or at most a few percent. In order to make an efficient use of patch antennas, it is necessary to investigate the theory of those.

2.2.2 Types of Patch Antennas

When the conductive structure is energized by a current flow in the circuit a standing wave is generated by the complex impedance structure of the antenna and an electric field is generated from the edge of the antenna. The electric field becomes a propagating electromagnetic wave, thus the functionality of an antenna is achieved. Almost all antennas work on this basic principle; microstrip patch antennas are no exception to this. Square, rectangular, dipole (strip) and circular microstrip patches are the most common because of analysis and fabrication, and their attractive radiation characteristics, especially low cross-polarization radiation. Microstrip dipoles are attractive because they inherently possess a large bandwidth and occupy less space, which makes them attractive for arrays. Rectangular patch antennas are the most popular for its simplicity of construction and good radiation characteristics. However, circular microstrip patch antennas are also used for the widest and most demanding applications. Dual characteristics, circular polarizations, dual frequency operation, frequency agility, broad band width, feed line flexibility, beam scanning can be easily obtained from circular patch antennas. Circular patch antennas come in many different forms, the most common form being a conductive structure printed on a dielectric substrate over a ground plane

[20]. Linear and circular polarization can be achieved with either single elements or arrays of microstrip antennas, arrays of microstrip elements, with single or multiple feeds , may also be used to introduce scanning capabilities and achieve greater directivities.

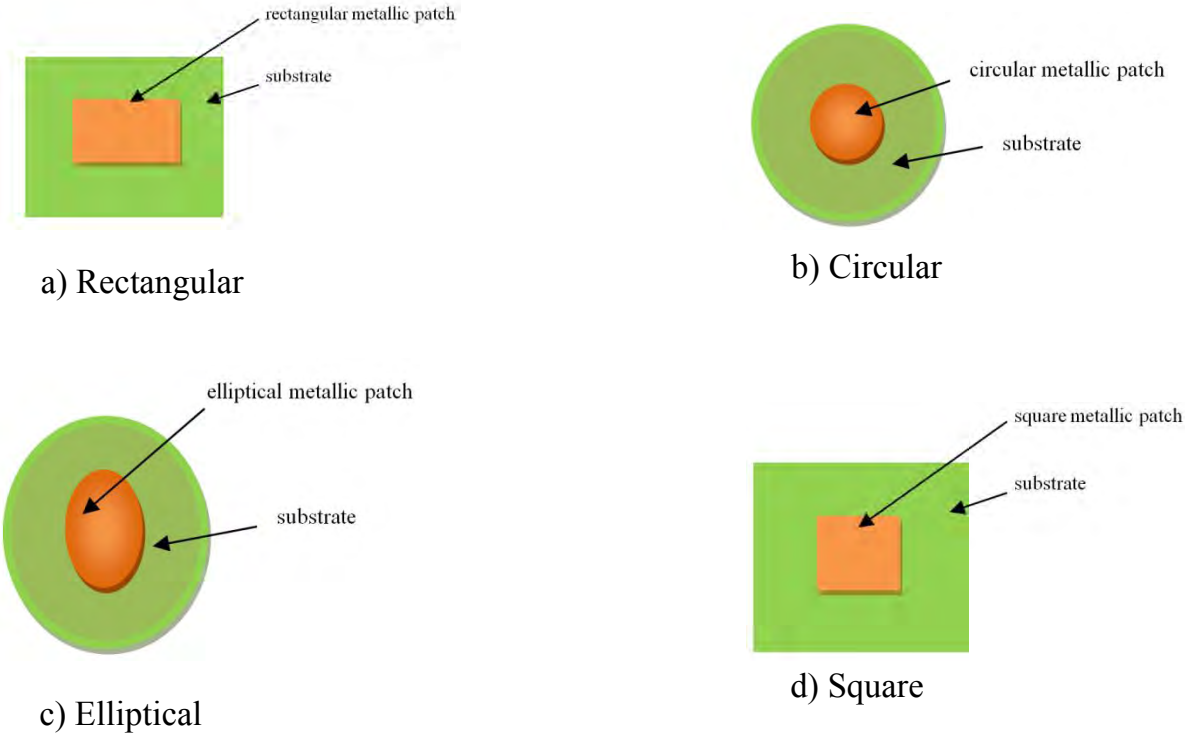

Fig. 2.9: Different types of patch antennas.

2.2.3 Mathematical Modeling of Rectangular Microstrip Patch Antenna: Transmission Line Model

There are many methods of analysis for microstrip antennas. The most popular models are the transmission-line [2], [21]; cavity [22], [23] and full wave [24] (which include primarily integral equations/ Moment Method). The transmission line model is the easiest of all, it gives good physical insight, but is less accurate and it is more difficult to model coupling. Rectangular patch antennas are very easy to analyze by using both transmission line and cavity models which are most accurate for thin substrates. Here transmission line model is discussed.

According to transmission line model, a rectangular microstrip patch antenna can be represented as an array of two radiating narrow apertures (slots), each of width W and height h, separated by a distance L. Basically the transmission line model represents the microstrip antenna by two slots, separated by a low-impedance Z_c and transmission line of length L shown in Fig. 2.10.

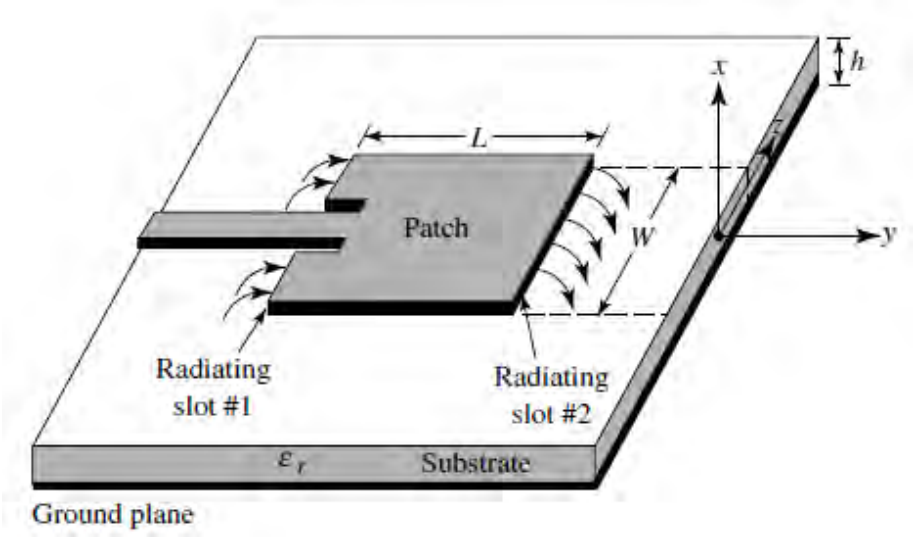

Fig. 2.10: A rectangular microstrip patch antenna with microstrip line feed [1].

Because the dimensions of the patch are finite along the length and width, the fields at the edges of the patch undergo fringing as shown in Fig. 2.10. The amount of fringing is a function of the dimensions of the patch and the height of the substrate. For the principal E-plane (xy plane) fringing is a function of the ratio of the length of the patch L to the height h of the substrate (L/h) and the dielectric constant ε_r of the substrate. Since for microstrip antennas L/h>>1, fringing is reduced; however it must be taken into account because it influences the resonant frequency of the antenna. Due to fringing fields, the effective dielectric constant of the patch substrate is reduced as Eq. (2.5). For low frequencies the effective dielectric constant is essentially constant. At intermediate

frequencies, its value begin to monotonically increase and eventually approach the values of the dielectric constant of the substrate described in Eq. (2.5) [1].

$$\varepsilon_{eff} = \frac{\varepsilon_r + 1}{2} + \frac{\varepsilon_r - 1}{2}[1 + 12\frac{h}{W}]^{-\frac{1}{2}} \tag{2.5}$$

Because of the fringing effects, electrically the patch of the microstrip antennas looks greater than its physical dimension. A very popular and approximate relation for the normalized extension of the length is given by Eq. (2.6) [1].

$$\frac{\Delta L}{h} = 0.412\frac{(\varepsilon_{eff} + 0.3)(\frac{W}{h} + 0.264)}{(\varepsilon_{eff} - 0.258)(\frac{W}{h} + 0.8)} \tag{2.6}$$

Since the length of the patch has been extended by ΔL on each side, the effective length of the patch becomes as Eq. (2.7) [1].

$$L_{eff} = L + 2\Delta L \tag{2.7}$$

For designing a rectangular microstrip patch antenna, we need to specify the dielectric constant (ε_r), resonant frequency (f_r) and thickness of the substrate (h). After that we need to determine the width (W) and length (L) of the patch by Eq. (2.8) and (2.9) [1].

$$W = \frac{1}{2f_r\sqrt{\mu_0\varepsilon_0}}\sqrt{\frac{2}{\varepsilon_r + 1}} \tag{2.8}$$

$$L = \frac{1}{2f_r\sqrt{\mu_0\varepsilon_0}\sqrt{\varepsilon_{eff}}} - 2\Delta L \tag{2.9}$$

ε_{eff} and ΔL are calculated from Eq. (2.5) and (2.6).

2.2.4 Feeding Methods

Microstrip Line Feed:

There are many configurations that can be used to feed microstrip antennas. The four most popular are the microstrip line, coaxial probe, aperture coupling, and proximity coupling [25–29]. The microstrip feed line is also a conducting strip, usually of much smaller width compared to the patch. The microstrip-line feed is easy to fabricate, simple to match by controlling the inset position and rather simple to model. However as the substrate thickness increases, surface waves and spurious feed radiation increase, which for practical designs limit the bandwidth (typically 2–5%).

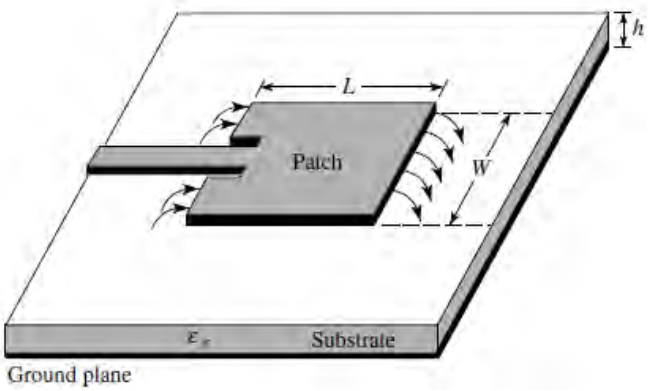

Fig. 2.11: Microstrip line feed [1].

In case of feeding with microstrip line, both edge feed (feed-line at the edge of patch) and inset feed (feed-line cut through the patch) methods are used. Basically, the transmission-line model shown in Fig. 2.10, represents the microstrip antenna by two slots, separated by a low-impedance Z_c and a transmission line of length L. Each radiating slot is represented by a parallel equivalent admittance Y (with conductance G and susceptance B). This is shown in Fig. 2.12.

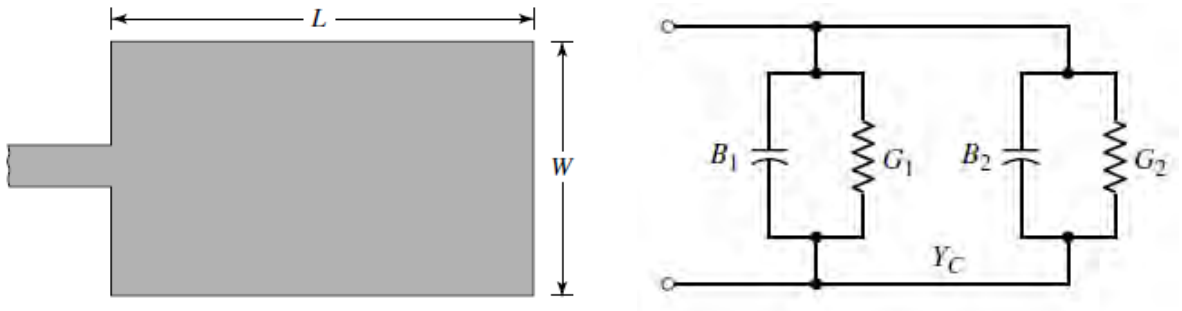

a) Rectangular patch b) Transmission model equivalent

Fig. 2.12: Rectangular microstrip patch and its equivalent circuit transmission line model [1].

The equivalent admittance of slot 1 can be written as in Eq. (2.10) [1].

$$Y_1 = G_1 + jB_1 \tag{2.10}$$

For a slot of finite width W,

$$G_1 = \frac{W}{120\lambda_0}[1 - \frac{1}{24}(k_0 h)^2], \frac{h}{\lambda_0} < \frac{1}{10} \tag{2.11}$$

$$B_1 = \frac{W}{120\lambda_0}[1 - 0.636\ln(k_0 h)], \frac{h}{\lambda_0} < \frac{1}{10} \tag{2.12}$$

Since slot 2 is identical to slot 1, its equivalent admittance is-

$$Y_2 = Y_1, G_2 = G_1, B_2 = B_1$$

The total resonant input admittance is real and is given by-

$$Y_{in} = Y_1 + Y_2 = 2G_1 \tag{2.13}$$

Since the total input admittance is real, the resonant input impedance is also real as in Eq. (2.14).

$$Z_{in} = \frac{1}{Y_{in}} = R_{in} = \frac{1}{2G_1} \tag{2.14}$$

Here mutual coupling between slot 1 and slot 2, i.e. G_{12} has been neglected since it is very small.

As shown by Eq. (2.11) and (2.14), the input resistance is not strongly dependent upon the substrate height h. In fact, for very small values of h, such that $k_o h << 1$, the input resistance is not dependent on h. It is also apparent from Eq. (2. 11) that the resonant input resistance can be decreased by increasing the width *W* of the patch. This is acceptable as long as the ratio of W/L does not exceed 2 because the aperture efficiency of a single patch begins to drop, as W/L increases beyond 2.

The resonant input resistance, as calculated by Eq. (2.14) is referenced at slot 1. However, it has been shown that the resonant input resistance can be changed by using an inset feed, recessed a distance y_0 from slot 1, as shown in Fig. 2.13(a). This technique can be used effectively to match the patch antenna using a microstrip-line feed.

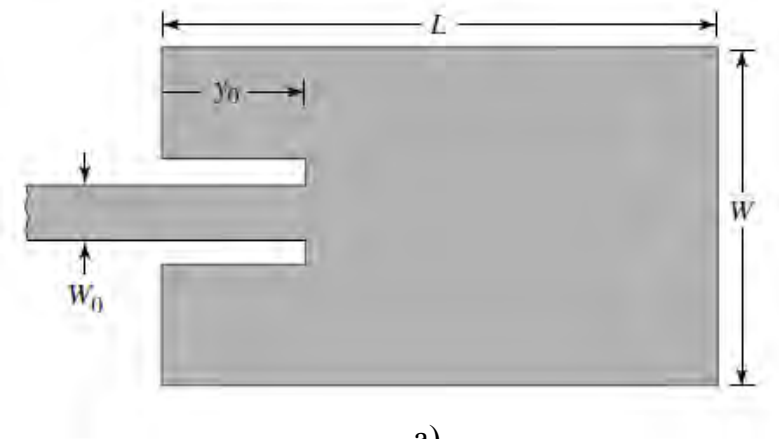

a)

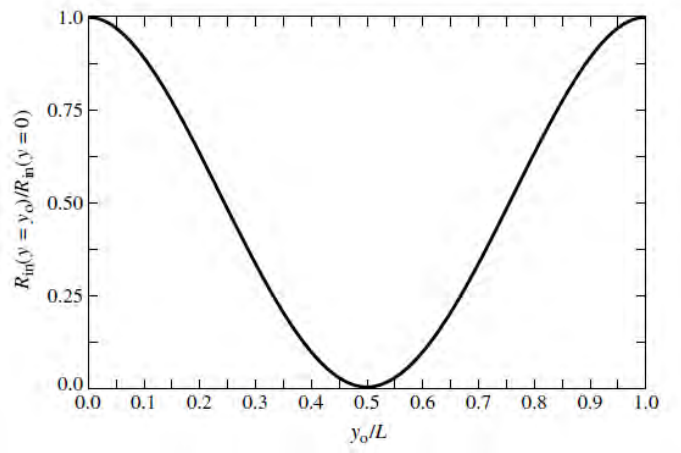

b)

Fig. 2.13: (a) Inset feed microstrip line,
(b) Normalized input resistance [1].

The characteristic impedance of the microstrip line feed is given by Eq. (2.15) and (2.16) [30].

$$Z_c = \frac{60}{\sqrt{\varepsilon_{reff}}} \ln[\frac{8h}{W_0} + \frac{W_0}{4h}], \frac{W_0}{h} \leq 1 \tag{2.15}$$

$$Z_c = \frac{120\pi}{\sqrt{\varepsilon_{reff}}[\frac{W_0}{h} + 1.393 + 0.667\ln(\frac{W_0}{h} + 1.444)]}, \frac{W_0}{h} > 1 \tag{2.16}$$

where W_0 is the width of the microstrip line.

Using modal expansion analysis, the input resistance for the inset feed is given approximately by Eq. (2.17).

$$R_{in}(y = y_0) = \frac{1}{2G_1}\cos^2(\frac{\pi}{L}y_0) = R_{in}(y = 0)\cos^2(\frac{\pi}{L}y_0) \tag{2.17}$$

It is apparent from Eq. (2.17) and Fig. 2.13(b) that the maximum value occurs at the edge of the slot ($y_0 = 0$) where the voltage is maximum and the current is minimum; typical values are in the 150–300 ohms. The minimum value (zero) occurs at the center of

the patch (y_0 = L/2) where the voltage is zero and the current is maximum. As the inset feed point moves from the edge toward the center of the patch the resonant input impedance decreases monotonically and reaches zero at the center. When the value of the inset feed point approaches the center of the patch (y_0 = L/2), the $\cos^2(\frac{\pi y_0}{L})$ function varies very rapidly; therefore the input resistance also changes rapidly with the position of the feed point. To maintain very accurate values, a close tolerance must be preserved.

Coaxial Feed:

Coaxial-line feeds, where the inner conductor of the coax is attached to the radiation patch while the outer conductor is connected to the ground plane, are also widely used. The coaxial probe feed is also easy to fabricate and match, and it has low spurious radiation. However, it also has narrow bandwidth and it is more difficult to model, especially for thick substrates (h > 0.02λ).

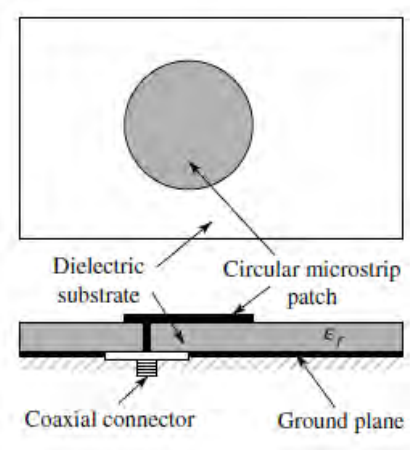

Fig. 2.14: Coaxial probe feed [1].

Aperture-coupled and Proximity-coupled Feed:

Both the microstrip feed line and the probe possess inherent asymmetries which generate higher order modes that produce cross-polarized radiation. To overcome some of these

problems, non-contacting aperture-coupling feeds, as shown in Fig. 2.15(a) have been introduced.

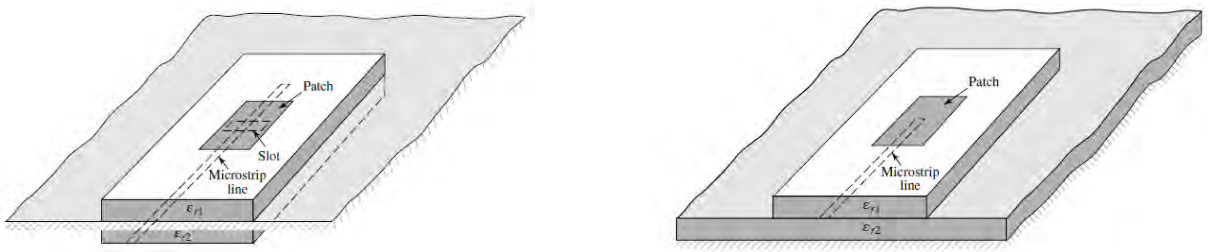

a) Aperture coupled feed b) Proximity coupled feed

Fig. 2.15: Typical feeds for microstrip antennas [1].

The aperture coupling is the most difficult of all four to fabricate and it also has narrow bandwidth. However, it is somewhat easier to model and has moderate spurious radiation. The aperture coupling consists of two substrates separated by a ground plane. On the bottom side of the lower substrate, there is a microstrip feed line whose energy is coupled to the patch through a slot on the ground plane separating the two substrates. Typically a high dielectric material is used for the bottom substrate, and thick low dielectric constant material for the top substrate.

The proximity coupling, shown in Fig. 2.15(b), has the largest bandwidth (as high as 13 percent), is somewhat easy to model and has low spurious radiation. However its fabrication is somewhat more difficult. The length of the feeding stub and the width-to-line ratio of the patch can be used to control the match

Chapter 3

Fabrication of Rectangular Patch Antennas

3.1 Introduction

Based on the theoretical background on antennas described in the previous chapter, the fabrication of rectangular patch antennas has been discussed in this chapter. Antenna fabrication has several steps which are often cumbersome and most of the time interdependent. In fact, a minimal error in the fabrication of one parameter can seriously affect the antenna characteristics those are related to that parameter. Therefore during fabrication, this factor must be taken care of to obtain the best performance from the theoretical modeling of an antenna. In this study, fabrication of three rectangular patch antennas (two loaded with plastic substrate, one loaded with barium titanate) for the operation in GSM band frequencies have been described. Rectangular patch antennas loaded with plastic substrate have been designed and fabricated for both GSM 900 MHz and 1800 MHz band frequencies, while barium titanate loaded patch antennas have been fabricated for GSM 1800 MHz frequency band.

3.2 Effect of Substrate Permittivity

Permittivity has both real and imaginary parts as shown in Eq. (3.1):

$$\varepsilon = \varepsilon_0 \varepsilon_r = \varepsilon' - j\varepsilon'' \tag{3.1}$$

The real part is responsible for the capacitive nature of the dielectric whereas, the imaginary part signifies the dielectric loss incurred due to misalignment of the dipoles in the dielectric material with the applied alternating electric field described by 'tan delta' function given by:

$$\tan\delta = \frac{\sigma_s + j\omega\varepsilon''}{j\omega\varepsilon'} \qquad (3.2)$$

where, σ_s is the conductivity of the dielectric

The value of the permittivity plays an important role in patch antenna radiation efficiency and frequency. The smaller the permittivity is, the more "bowed" the fringing fields become; they extend farther away from the patch. Therefore, using a smaller permittivity for the substrate yields better radiation. In contrast, a high value of permittivity of the substrate causes the fields to become more tightly contained and thus yields less fringing and consequently less radiation. This type of substrate is suitable for microstrip transmission line where no power is supposed to be radiated.

3.3 Substrate Fabrication and Analysis

Sheets of plastic and barium titanate discs have been used as the substrates for the patch antennas. These substrates were not available in suitable form for patch antenna use. So, they were either prepared or fabricated in laboratory. Later antenna length, width and other parameters were fixed according to the permittivity of the substrates. The fabrication process for both the dielectric substrates are described in this chapter.

3.3.1 Capacitance Measurement and Permittivity Calculation of Plastic Substrate

In literature, there are several methods available for the permittivity measurement of dielectrics [31, 32]. Irezalana mpna mpmin Glass and Ceramic Laboratory of BUET was used in this research rol the calculation of permittivity of plastic and barium titanate substrate from their capacitances. A corner portion from a rectangular plastic slab having a thickness of 8 mm was cut off obliquely in carpentry shop to a nka it m three dimensional tliangular shmnaas shown in Fig. 3.1(a) . Then it was placed inside the probe of impedance analyzer at the position shown in Fig. 3.1(b). The instrument was calibrated

properly before that. The impedance analyzer available in the lab could measure the capacitance of dielectric material placed between its probe over the frequency range from 10 Hz to 10 MHz. Later, real permittivity was calculated from the measured capacitance using Eq. (3.3). On the impedance analyzer screen shown in Fig. 3.1(c), the green curve is the capacitance of the dielectric and the yellow curve is the loss tangent of the material. It is seen that on the range from 10 Hz-10 MHz, the capacitance does not vary that much except some fluctuations at the beginning. From the yellow curve it is also seen that the loss tangent of the material due to alternating electric field is close to zero. For this reason, the dielectric loss of plastic substrate has been neglected in this measurement process. For the purpose of a better illustration of the dielectric nature of plastic, the capacitance of it is plotted separately in MATLAB in Fig. 3.3 from which the real part of the permittivity has been calculated later.

a) Plastic substrate cut at a suitable shape

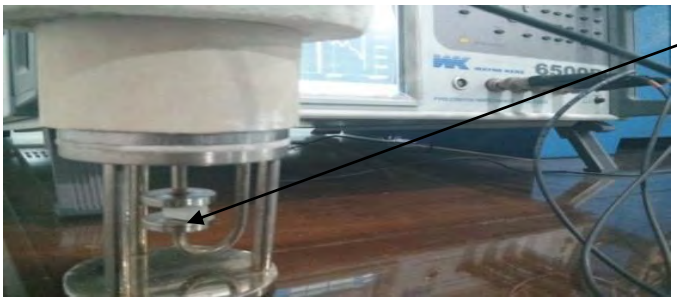

b) Impedance analyzer probe (side view)

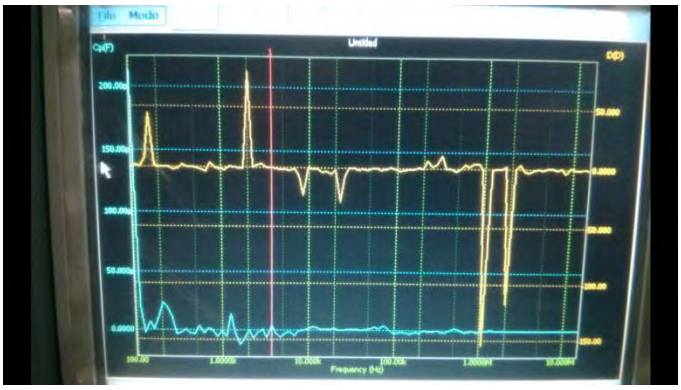

c) Capacitance versus frequency plot in the screen of impedance analyzer (green curve); loss tangent versus frequency (yellow curve)

Fig. 3.1: Permittivity measurement process of plastic substrate.

Impedance analyzer measures the capacitive impedance between the probes due to a dielectric material. From that result, we can get the permittivity at different frequencies. The top view of the dielectric material of Fig. 3.1(a) can be redrawn as in Fig. 3.2 for proper mathematical modeling.

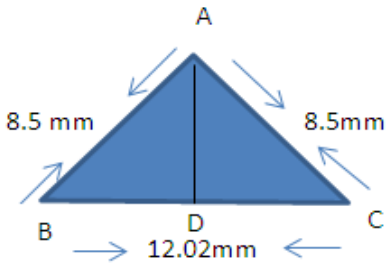

Fig. 3.2: Schematic of the dielectric substrate obliquely cut from a rectangular slab (2-D view).

From Fig. 3.2,

AB=8.5 mm

AC= 8.5 mm

Since the dielectric is a corner portion of a larger rectangular solid, we can consider angle ∠BAC equal to 90̊.

$$\text{therefore, } BC = \sqrt{AB^2 + AC^2} = 12.02mm \text{ , } BD = \frac{BC}{2} = 6.01mm$$

$$AD = \sqrt{AB^2 - BD^2} = 6.01mm$$

$$\text{So, the area of triangle ABC, } A = \frac{1}{2} \times AD \times BC = 36.09\ mm^2$$

The capacitance data of the dielectric obtained from impedance analyzer is shown in Table -3.1

Table-3.1: Measured capacitances of plastic substrate

Frequency	Measured Capacitance (fF)
10 Hz	130
100 Hz	130
1kHz	125
10kHz	125
1MHz	125
10 MHz	125

The data of Table 3.1, plotted in MATLAB [33] is shown in Fig. 3.3. Considering the constant value of the capacitance as 125fF at higher frequency, relative permittivity has been calculated.

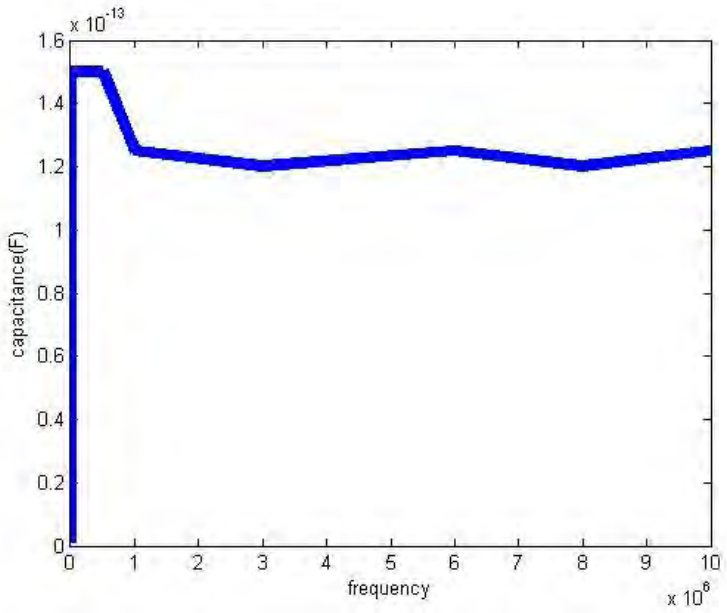

Fig. 3.3: Capacitance versus frequency plot for plastic substrate.

The formula for capacitance is: $C = \frac{\varepsilon_0 \varepsilon_r A}{d}$ (3.3)

Here, C= 125fF, A= 36.09mm^2, d= 8 mm and ε_r is the relative permittivity.

therefore, $\varepsilon_r = \frac{Cd}{\varepsilon_0 A} = 3.101$

This is the calculated permittivity for the substrate only. However when used as substrate in patch antenna, the effective permittivity of dielectric material changes due to fringing effect of electric field which will be discussed in Chapter 4.

3.3.2 Barium Titanate Substrate Fabrication Process in Laboratory

Barium titanate is not available as solid substrate form. It is usually found in powdered form [34]. Suitable shaped barium titanate substrate for patch antenna application has to be fabricated in the laboratory by the processing of barium titanate powder with other

chemicals. However, due to the cylindrical shape of the hydraulic machine, only circular or disc shaped substrate of a particular diameter can be fabricated in the laboratory. The whole fabrication process was done in the Glass and Ceramic department of BUET. At first 98% barium titanate and 2% binder were mixed properly. This mixture was placed inside hydraulic piston under 20 N force. Barium titanate discs were formed with a radius of 15 mm and thickness of 4 mm. 3-4 barium titanate discs were fabricated. These barium discs were then placed at high temperature (around 1300℃) for sintering process in the oven for about 2 hours. After sintering, the substrates became rigid and usable as antenna substrate. Tha whora nlonass is showp be m ta a glmnh ipFig. 3.4.

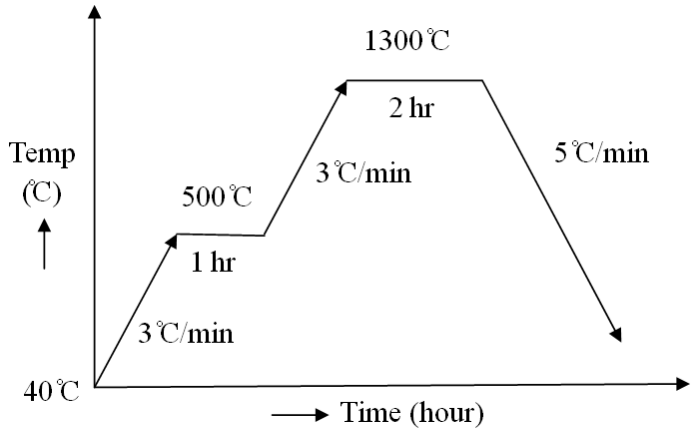

Fig. 3.4: Barium titanate fabrication graph with time.

3.3.3 Capacitance Measurement and Permittivity Calculation of Barium Titanate Substrate

After fabrication, the capacitance of barium titanate substrate was measured in the impedance analyzer the same way as in section 3.3.1. A barium titanate disc was placed between the probes of the impedance analyzer shown in Fig. 3.5. Here also the

capacitance of the substrate falls with frequency and then settles at almost a constant value (green curve).

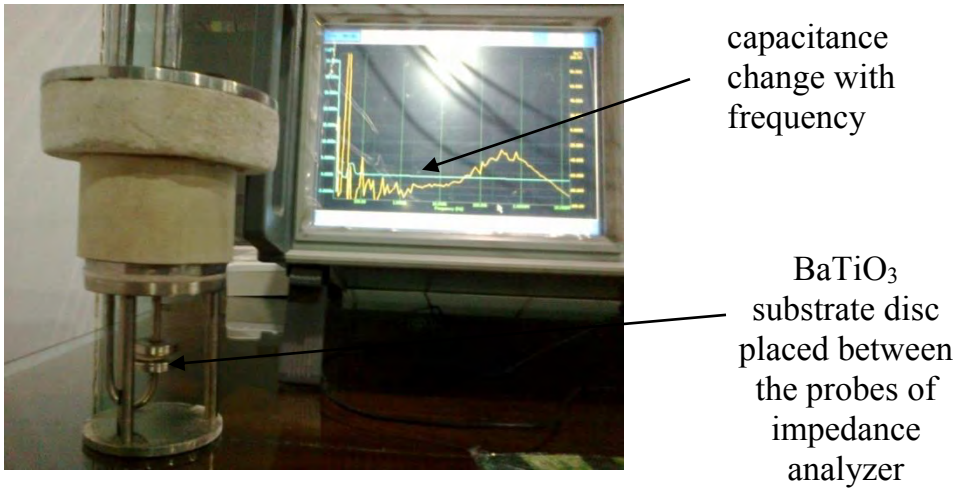

Fig. 3.5: Permittivity measurement process of barium titanate substrate.

The measured capacitance data of barium titanate is shown in Table 3.2 and plotted in MATLAB (Fig. 3.6).

Table-3.2: Measured capacitances of barium titanate substrate

Frequency	Measured Capacitance (pF)
10 Hz	18
100 Hz	13
1kHz	13
10kHz	13
1MHz	13
10 MHz	13

The constant value of capacitance is taken as 13 pF. This value has been used in later calculation.

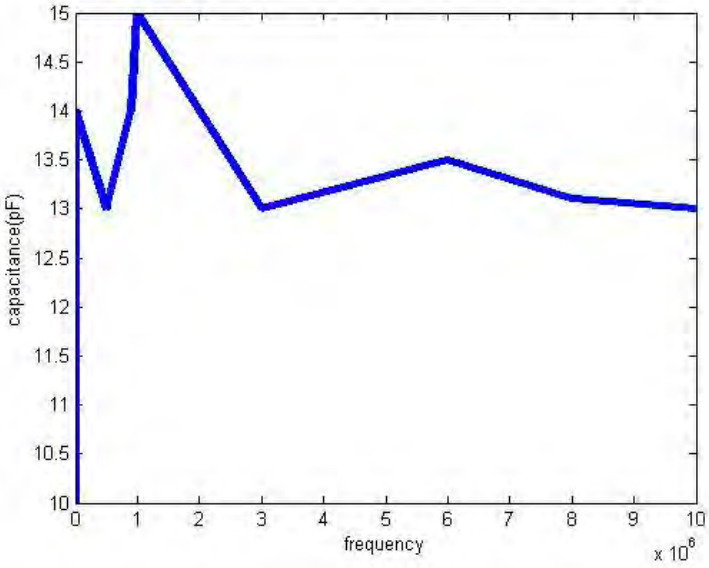

Fig. 3.6: Capacitance versus frequency plot for barium titanate substrate.

Using Eq. (3.3) again, the permittivity for barium titanate is calculated.

here, C=13 pF

Radius of the Barium Titanate disc, r= 7.5 mm

Area of the circular disc, A= $\pi r^2 = 176.71$ mm^2

Thickness of the disc, d= 4 mm

Therefore, permittivity, $\varepsilon_r = \dfrac{Cd}{\varepsilon_0 A} = 32.23$

This value of permittivity has been used later for fixing the dimensions of the patch and other parameters.

3.4 Antenna Fabrication Procedure

3.4.1 GSM 900 MHz Patch Antenna Loaded with Plastic Substrate

All the parameters of the antenna were fixed after measuring the permittivity of the plastic substrate material mentioned in section 3.3. The substrate dimension was 160 mm×230 mm with a thickness of 8 mm. Glue was used to form a rigid sandwiched structure as shown in Fig. 3.6. A 50 ohm matched coaxial cable was used to feed the antenna through a microstrip transmission line. From Eq. (2.5)-(2.9), the following parameters are calculated-

Length of the patch antenna = 94.66mm

Width of the patch antenna= 116.4mm

Effective permittivity, ε_{eff} = 3.06

Effective length , L_{eff} = 87mm

From Eq. (2.16), transmission line feed width, W_f = 19.6 mm

From Eq. (2. 17), length of the feed inside the patch, F_i= 28.61 mm

Transmission line feed length, L_f = 72.12 mm

Gap between patch and microstrip transmission Line, G_{pf}= 2 mm

Later rectangular patch antenna at 900 MHz was constructed using the above calculations as shown in Fig. 3.7. Measurement and simulation results of the antenna agree quite satisfactorily which will be discussed in chapter 4 and 5.

Fig. 3.7: Top View of GSM 900 MHz patch antenna loaded with plastic substrate.

3.4.2 GSM 1800 MHz Patch Antenna Loaded with Plastic Substrate

A GSM 1800 MHz patch antenna was fabricated by following the same procedure as in section 3.4.1. Here all the dimensions of the antenna were close to half of the previous case, but the thickness of the substrate was kept same as before, i.e. 8 mm. It is advisable to maintain the thickness of substrate less than 0.02×lamda to reduce the effects of surface waves [35, 36]. Other necessary parameters were calculated from Eq. (2.5)- (2.9) which are given below-

Patch length, L= 44 mm

Patch width, W= 60 mm

Plastic substrate length, L= 90 mm

Plastic substrate width, W= 180 mm

Substrate thickness, h= 8 mm

Effective length, L_{eff} = 40 mm

From Eq. (2.16),

Transmission line feed width, W_f = 19.6 mm

From Eq. (2. 17),

Length of the feed inside the patch, F_i= 15 mm

Gap between microstrip line, G_{pf}= 2 mm

The above calculated parameters were used for antenna fabrication. However, it is mentionable here that in order to decrease loss and maintain symmetry at 1.8 GHz, the width of the trasmission line was chosen to be 5 mm instead of its calculated value of 19.6 mm. The constructed antenna is shown in Fig. 3.8. The experimental and simulation results are discussed in the next two chapters.

Fig. 3.8: Top View of GSM 1800 MHz patch antenna loaded with plastic substrate.

3.4.3 GSM 1800 MHz Patch Antenna Loaded with Barium Titanate Substrate

By using barium titanate as the substrate, a GSM 1800 MHz patch antenna was fabricated. Due to the high dielectric permittivity of barium titanate, all the dimensions of

the antenna became very small. For this reason, it was really very difficult to implement the whole design. By following the same procedure as in section 3.4.1 and 3.4.2, all the dimensions of the antenna were calculated, but the thickness of the barium titanate substrate was kept 4.5 mm as it was fixed during substrate fabrication. The fabricated antenna is shown in Fig. 3.9 below.

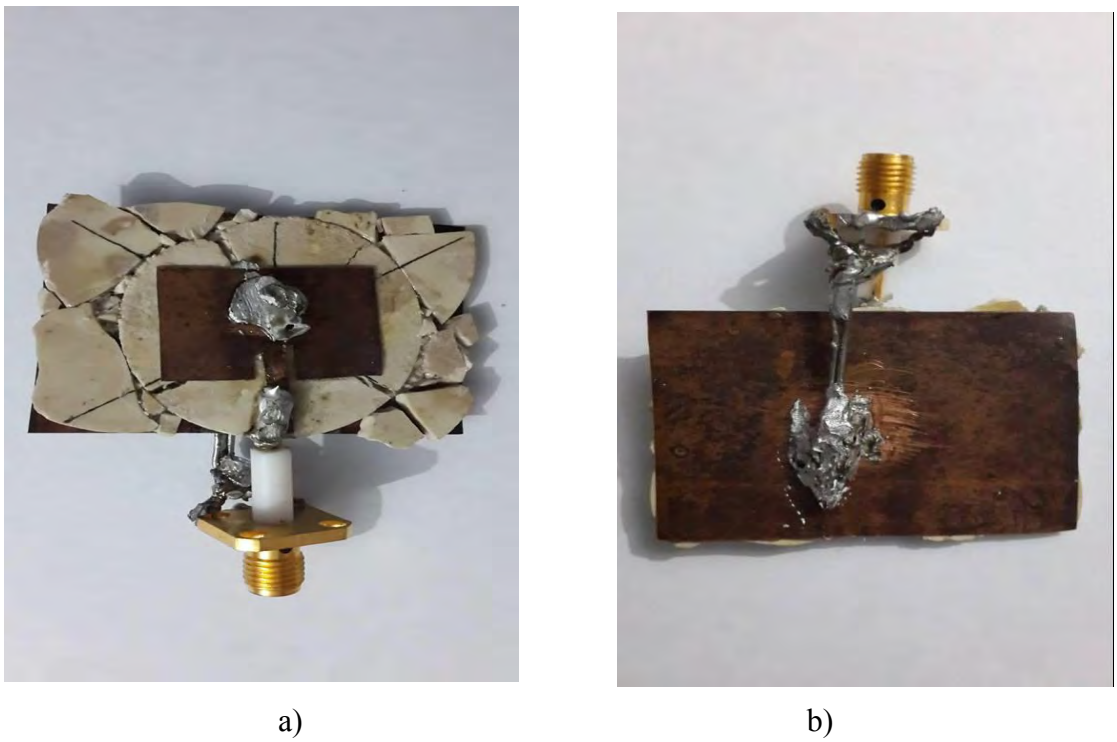

a) b)

Fig. 3.9: GSM 1800 MHz rectangular patch antenna loaded with barium titanate substrate (a) top view (b) bottom view.

Other necessary parameters were calculated from Eq. (2.5)- (2.9) which are given below-

Patch length, L= 14.7 mm

Patch width, W= 28.9 mm

Effective length, $L_{eff} \cong 12mm$

From Eq. (2.16),

Transmission line feed width, $W_f = 1$ mm

From Eq. (2. 17),

Length of the feed inside the patch, $F_i = 3$mm

Gap between microstrip line, $G_{pf} = 1$mm

Chapter 4

Experimental Investigation of the Fabricated Antennas

4.1 Introduction

The patch antennas were fabricated as described in Chapter 3 and were then taken to the lab for experimentation. Two antennas loaded with plastic substrate and one loaded with barium titanate substrate were tested in laroratory. The testing and measurement procedure will be discussed in this chapter. Antenna testing is usually done in anechoic chamber so that the effects of spurious radiation and reflections are minimized [37]. An anechoic chamber is a room designed to completely absorb reflections of either sound or electromagnetic waves. As it was not available, the tests of the antennas were done in the microwave laboratory of BUET and University of Asia Pacific (UAP).

Due to the inavailability of network analyzer, it was also not posible to investigate the return loss (s-parameter) of the fabricated antennas. Instead, the received power data by the adjacent receiver antenna was used to describe the resonant characteristics of the transmitter antenna since a sudden peak in received power by the receiver antenna indicates the resonance of transmitter antenna of the nearby viscinity at that frequency. Moreover, the available oscillator in the BUET Microwave Laboratory could feed the antenna with signals only in the frequency range between 1200 MHz to 1900 MHz. For this reason, it was also not possible to observe the received power level by the receiver antenna at 900 MHz there. Radiation pattern and received power level at 900 MHz were measured at UAP laboratory while radiation patterns at 1800 MHz and received power level by the receiver antenna systems in 1200 MHz-1900 MHz frequency range were

measured at BUET. Tha tala 'sigpmrstlapgth' a amsuh ip B mp Ba hmsbaap usa to lanlasapt lm imtiop mtalps mp lanaiva no wal ravar lasnantivare ip thasa axnaliaapts.

4.2 Experimental Set-up for Antenna Measurement

At first a 900 MHz rectangular patch antenna was fabricated for experimental investigation purpose since it is larger in shape. A larger shaped antenna at a lower frequency is supposed to cause less variation in antenna performance with the unintentional changes in its parameters. So while comparing the performance of fabricated antenna from its theoretical modelling, experiment with larger shaped antennas is always advisable [38]. The radiation characteristics of the 900 MHz patch antennna at 900 MHz was tested in the Microwave Laboratory of UAP. After that a smaller antennna loaded with similar plastic dilectric was fabricated to operate at GSM 1800 MHz frequency. Its radiation performance was investigated in the Microwave Laboratory of BUET. Satisfactory performance was obtained in the radiation analysis of the patch antenna.

However, these two antennas were bulky and of larger in shape due to lower value of the dielectric constant of the underneath substrate. In today's antenna communcation, smaller sized path antennas are preferable [39]. But in order to fabricate a smaller sized patch antennna at the same desired frequency, the permittivity of the underneath substrate has to be high which usually causes a lesser gain. So a trade off has to be made between size and gain of the patch antenna. Barium titanate has a very high permittivity [40]. Although its fabrication process is very cumbersome, still it is possible to fabricate in the laboratory with the current facilities availabe in BUET. That is why, this substrate was used to fabricate a smaller sized patch antenna at the desired GSM 1800 MHz frequency. Although the gain performance of this antenna was not so good compared to previously reported antennas loaded with plastic dielectric, still appreciable radiation performance at the first order mode was obtained with a reduced sized radiator.

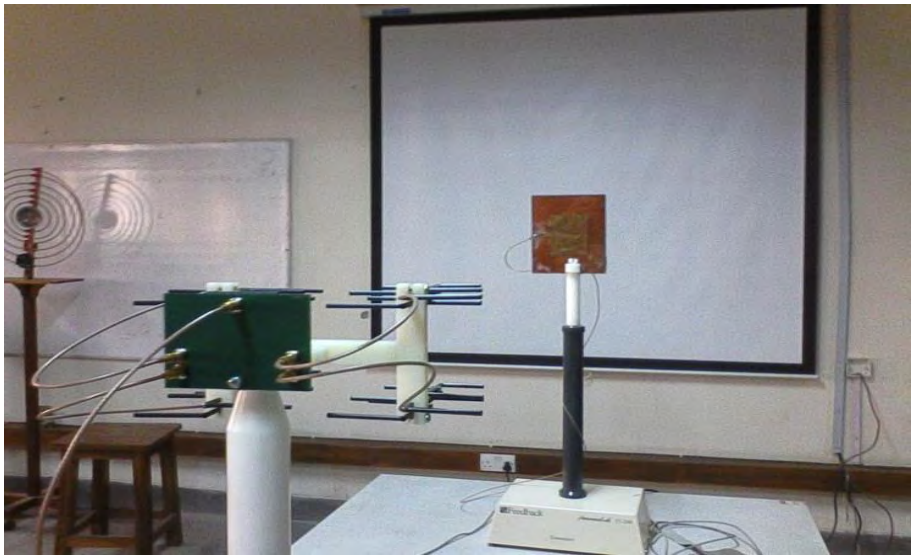

Fig. 4.1: Experimental set-up for antenna testing at BUET Microwave Laboratory.

The fabricated antennas were at first tested in the Microwave Laboratory of BUET. The experiental set-up with a 1800 MHz transmitter patch antenna is shown in Fig. 4.1. Due to reciprocity, it is desirable to use the same type of antenna as the receiver [41]. However, in the laboratory a log-periodic antenna array interfaced with the computer and placed at a distance of about 2-3 meters from the trasmitter patch antenna, was used as the receiving antenna. The gain and other radiation performances of log-periodic antennnas are less dependant on frequency; these are also called frequency indepenedent antennas [42]. Frequency independent antennas are a particular class of wideband antennas, which were first studied by Rumsey [43]. These are the antennas that have the geometry that are completely specified by angles. Despite using this antenna system, it was possible to measure the received signal from the transmitting rectangular patch antenna with good accuracy. The whole antenna system was interfaced through 4nec2 sofware in order to display the test results in the computer screen [44].

4.3 Experimental Results

4.3.1 Rectangular Patch Antenna at 900 MHz Loaded with Plastic Substrate

The first part of experiment at 900 MHz frequency for the GSM 900 MHz patch antenna was performed at UAP Microwave Laboratory. The experimental set up was exactly similar to Fig. 4.1. However, as the receiver antenna here a 1 GHz rectangular patch antenna was interfaced via Antenna Trainer System (ATS) module [45]. From Fig. 4.2, it is evident that the received power level shows a drastic increase in between 800 MHz to 900 MHz. Since this antenna was primarily supposed to be resonant at 900 MHz, it can be assumed that the bump of 20.79 dBm in received power level at this frequency region is due to the fundamental resonant mode of the nearby 900 MHz transmitter patch antenna.

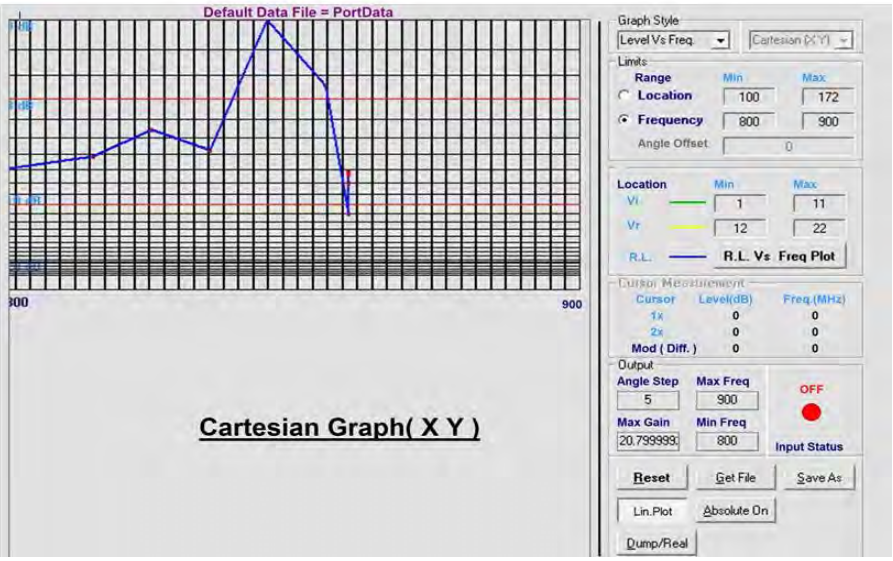

Fig. 4.2: Received power level versus frequency graph observed in ATS.

It is necessary to observe the radiation pattern of the patch antennas at the desired frequency to term it as a good radiator at that frequency. Polar plot of radiation pattern at phi plane is shown in Fig. 4.3. Patch antennas are supposed to be omnidirectional [46] in

azimuthal direction (phi plane); that is why, at the fundamental resonat mode of the fabricated patch antenna this result is not that satisfactory. This might be due to inconvenient laboratory set up, reflection of transmitted signal from the side walls in the laboratory, spurious signals etc. as the experiment was not performed in anechoic chamber.

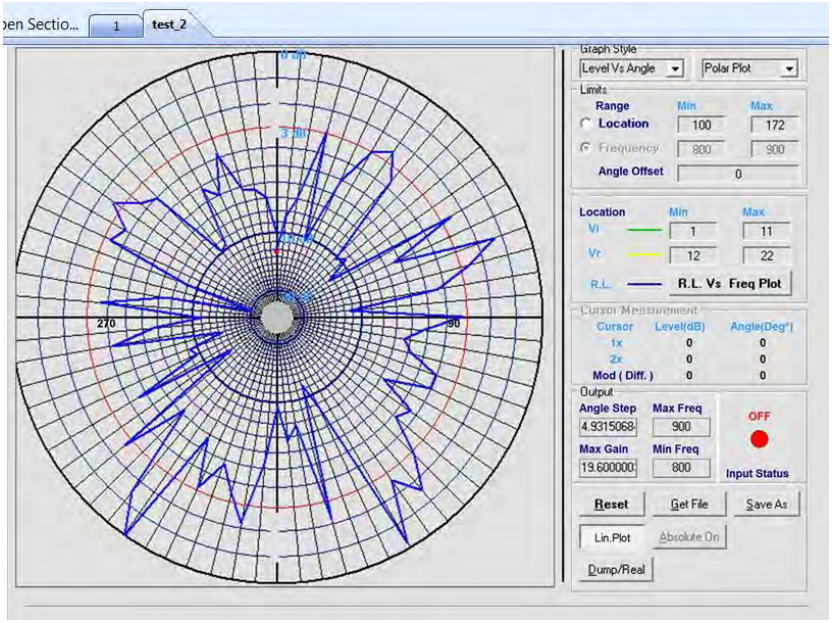

Fig. 4.3: Radiation pattern at phi plane for GSM 900 MHz patch antenna loaded with plastic substrate at 900 MHz.

After observing the radiation pattern of the fabricated patch antenna at 900 MHz, it was advised to observe its radiation pattern at its second order mode at 1800 MHz. However, at the Micowave Laboratory of UAP, it was not possible since the available oscillator there could sweep frequency from 0 to 980 MHz. So, in order to investigate the radiation pattern of the 900 MHz patch antenna at its second order mode which may be close to 1800 MHz, experiment was done in BUET Microwave lab and experimental set up mentioned in section 4.2 at BUET Microwave Laboratory was used. The experiment was performed twice (green and blue curve of Fig. 4.4). Almost same type of pattern was

obtained in both the ocasions. However, while observing its 2 dimesional normalized radiation pattern at 1794 MHz in theta plane, prominent side lobes were observed apart from two primary lobes. The high power level of the side lobes can be attributed to reflection, scattering and some minor flaws in fabrication process**.**

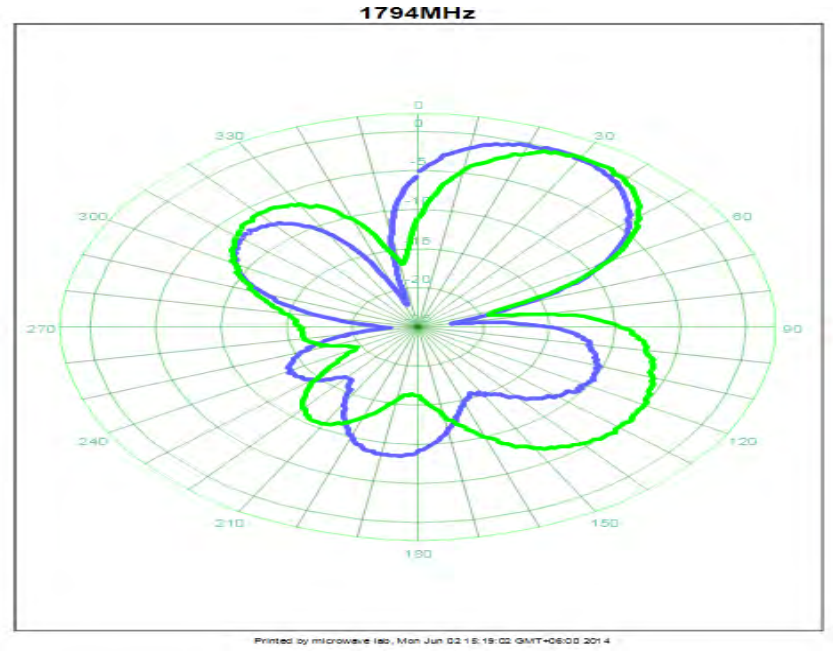

Fig. 4.4: Normalized radiation pattern at theta plane for GSM 900 MHz patch antenna loaded with plastic substrate at 1794 MHz (green and blue curves represent the 1st and 2nd trial of experiment).

4.3.2 Rectangular Patch Antenna at 1800 MHz Loaded with Plastic Substrate

After testing the 900 MHz patch antenna, 1800 MHz patch antenna was also tested. Using the set-up described in section 4.2, the signal strength detected by the nearby receiver antenna at the frequency range 1200 MHz-1900 MHz was measured. The obtained data is shown in Table- 4.1, which is plotted in MATLAB as in Fig. 4.5.

Table-4.1: Frequency versus signal strength

Frequency (MHz)	Signal Strength (dBm)
1200	-7.6
1300	-5.8
1400	-4.9
1500	-3.2
1600	-2.1
1700	-0.2
1800	14.9

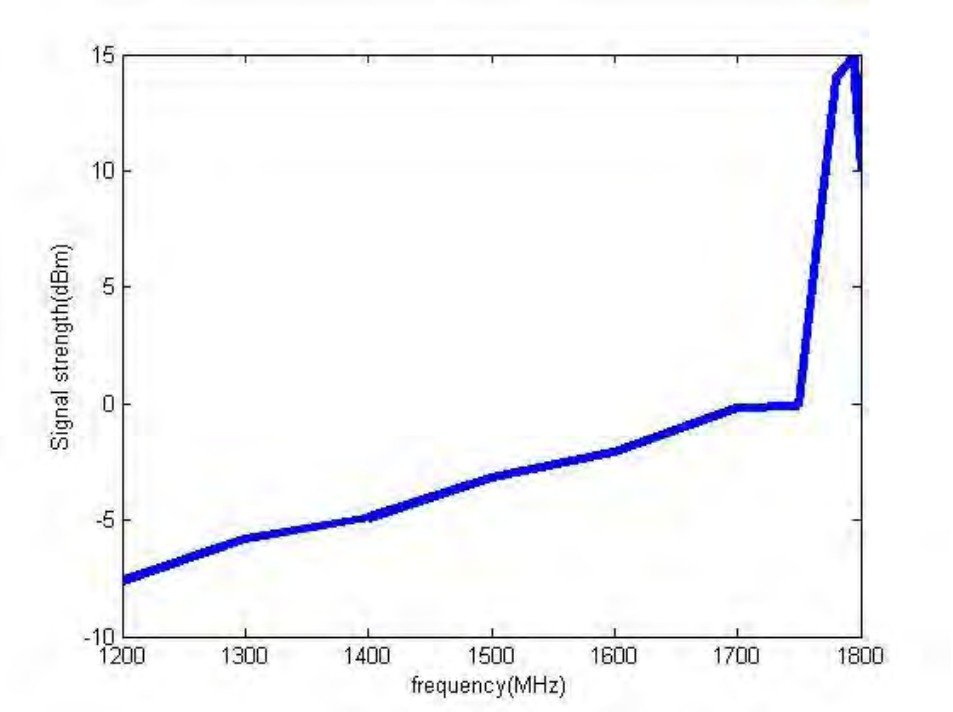

Fig. 4.5: Received power versus frequency graph for 1800 MHz plastic loaded patch antenna plotted in MATLAB.

It is seen that the signal strength measured in dB shows a peak of 14.9 dBm at a frequency of 1794 MHz. This is due to the fundamental resonant mode of 1800 MHz

transmitter patch antenna near that frequency. After that the radiation pattern of the patch antenna was measured in theta plane. Some of those data are shown in Table- 4.2.

Table-4.2: Angle versus signal strength

Angle (theta) in degrees	Signal strength (dB)
0	7.11
60	3.73
90	0.62
180	0.10
300	2.69
359	7.10

The normalized data plotted in 4nec2 software is shown in Fig. 4.6. It shows a very good broadside radiation with little side lobes.

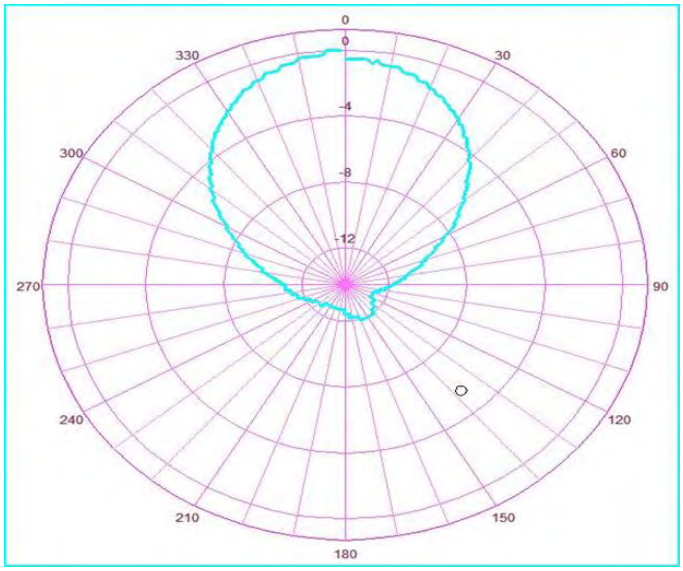

Fig. 4.6: Normalized radiation pattern in theta plane at 1794 MHz for 1800 MHz plastic loaded patch antenna.

4.3.3 Rectangular Patch Antenna at 1800 MHz Loaded with Barium Titanate Substrate

Patch Antennas fabricated with plastic substrate are bulky and less portable. A smaller sized patch antenna which can tune the same 1800 MHz frequency can be more efficient. But, in order to reduce the size of the patch antenna, a substrate with a high value of permittivity has to be used. Barium Titanate can be a good substrate in this case. Considering this factor, a patch antenna loaded with barium titanate at 1800 MHz was constructed and tested in the Microwave Laboratory of BUET. The antenna was rotated along theta plane and data were taken. Some of the measured data are given in Table-4.3. Although the received signal strength from this antenna was not that good compared to plastic loaded patch antenna, still its radiation characteristic showed a better directivity than the former case. Its slightly tilted main lobe with very negligible side lobes was clearly visible.

Table-4.3: Angle versus signal strength

Angle (theta) in degrees	Signal strength (dB)
0	0.68
60	3.53
90	0.62
150	4.3
180	1.19
240	5.87
270	2.23
330	0.68

In Fig. 4.7, normalized radiation pattern in vertical plane has been shown. It shows a good directive radiation in broadside, which is desirable from a patch antenna radiating near its fundamental radiating mode. However, there are some discontinuities, tilt and

bumps in the polar plot at some points. Minor flaws in fabrication and non-ideal measurement environment may be the reasons for this.

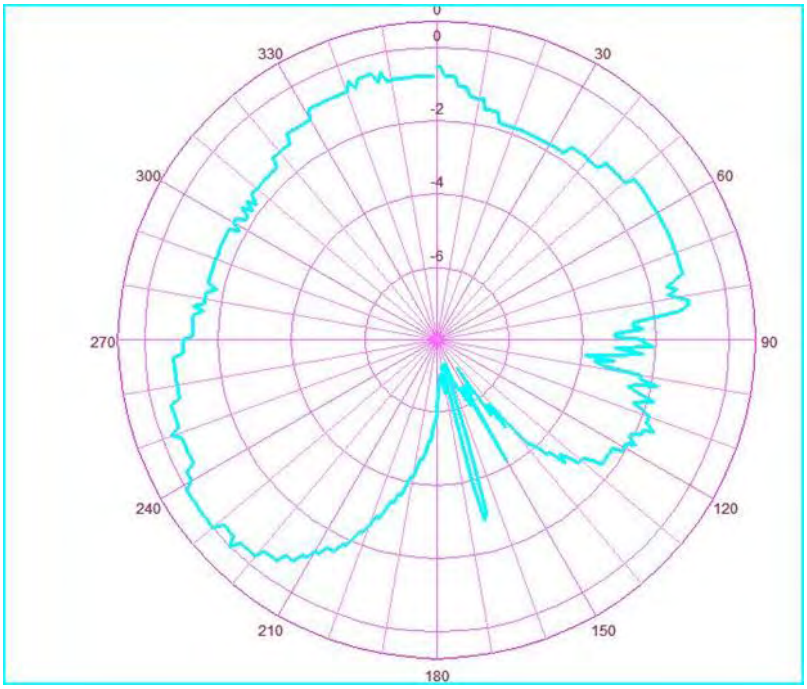

Fig. 4.7: Normalized radiation pattern in theta plane at 1793 MHz for barium titanate loaded patch antenna

The experimenal results of this section were later verified by simulations which will be discussed in chapter 5.

Chapter 5

A Comparative Study of Experimental and Simulation Results

5.1 Introduction

The performance of antennas or any other type of radiators can be termed appropriate only when their experimental and simulation results agree well. That is why, it is always necessary to verify the experimental results of antenna with its simulation. In most of the antenna research, antennas are fabricated based on its simulation analysis; then they are tested and compared [47]. However, in this research, this was done in reverse order, i.e., at first the antennas were fabricated and tested, then their performance were compared with their simulation results. Here High Frequency structural Simulator (HFSS) software was used for simulation which provides accurate simulation results of microwave circuits considering realistic environment [48]. Initially, all the antennas were drawn according to their geometric dimensions as calculated from their mathematical equations and later those were simulated. At the very beginning of the research, CST Microwave Studio software was also used for verification of the results [49]. In this section, simulation results obtained in HFSS software will be presented and discussed. At the end of this section, a comparative study between experimental and simulation results has also been done.

5.2 Simulation Results of Antennas

5.2.1 GSM 900 MHz Patch Antenna Loaded with Plastic Substrate

A 900 MHz rectangular patch antenna was drawn in HFSS exactly maintaining the dimensions of its fabricated prototype as shown in Fig. 5.1. Lumped port was used to feed the antenna through a microstrip line.

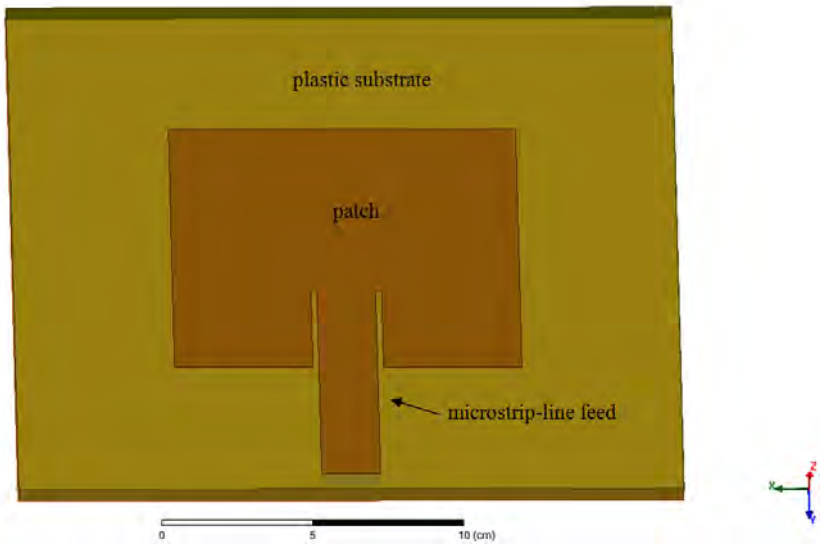

Fig. 5.1: 900 MHz patch antenna loaded with plastic substrate drawn in HFSS Software.

Frequency sweep was performed from 500 MHz to 2000 MHz to observe the s-parameter (s_{11}) or reflection coefficient of the antenna. From the s-parameter of the antenna (Fig. 5.2), it is evident that although there are some notches and fluctuation in the value of reflection in the aforementioned frequency range, good resonance occurs at 0.87 GHz which is 1st order TM mode). In the 2nd order TM resonance modes, some notches are also obtained from 1.4 GHz to 1.8 GHz.

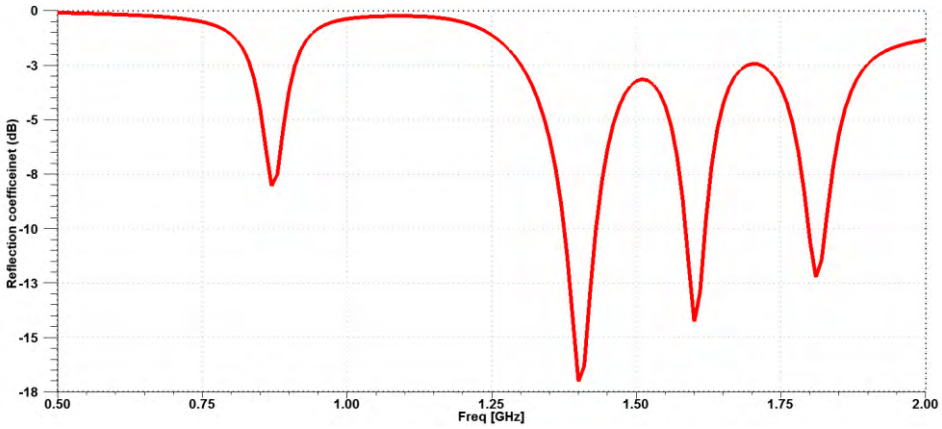

Fig. 5.2: S-parameter of 900 MHz patch antenna loaded with plastic substrate.

In order to term any radiator good, we need to investigate the radiation patterns of the antennas at the resonant frequencies alongside its resonance analysis. In Fig. 5.3, the radiation pattern at the fundamental 1st order mode of the antenna is shown. It is seen from the 3-D radiation pattern at Fig. 5.3(a) that total gain is 7.41 dB in the broadside direction which is quite good for GSM applications.

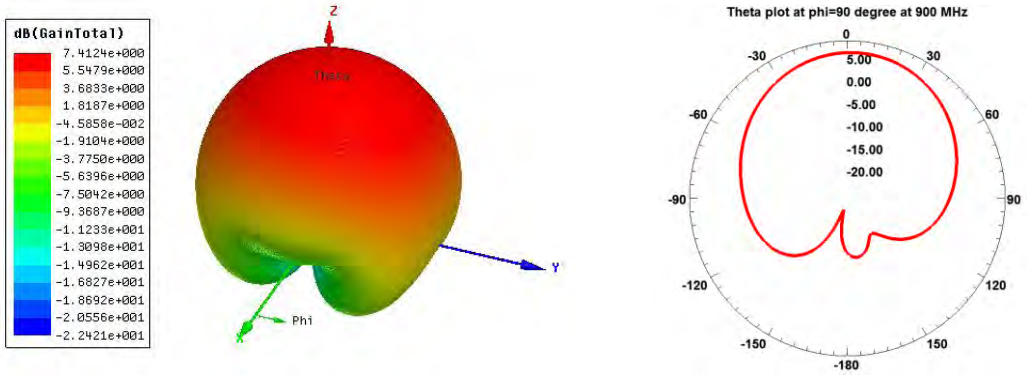

(a) (b)

Fig. 5.3: Radiation patterns of the 900 MHz plastic loaded patch antenna at 900 MHz (a) 3-D radiation pattern (b) 2-D radiation pattern in theta plane at phi=90°.

For further investigation, the radiation pattern was also investigated at one of the second order modes at 1.63 GHz which is shown in Fig. 5.4. It is seen that at far-field, the main beam is splitted into two primary lobes which satisfies the characteristics of the second order mode in patch antennas.

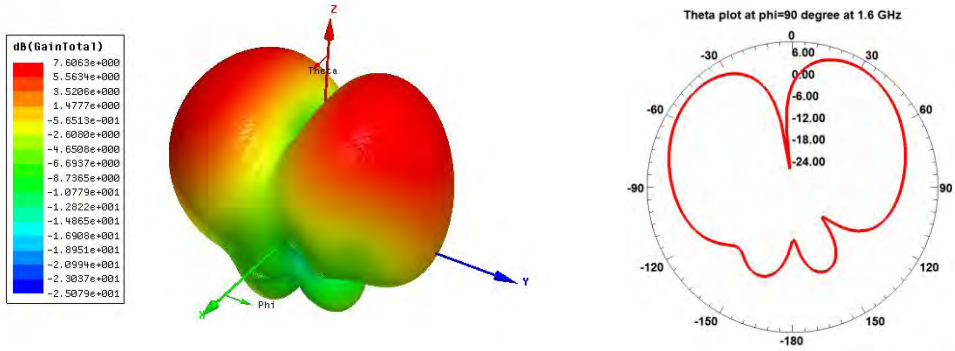

(a) (b)

Fig. 5.4: Radiation pattern of 900 MHz plastic loaded patch antenna at 1.6 GHz, (a) 3-D radiation pattern (b) 2-D radiation pattern in theta plane at phi=90°.

5.2.2 GSM 1800 MHz Patch Antenna Loaded with Plastic Substrate:

Using the same method as in section 5.2.1, another antenna at GSM 1800 MHz frequency band was drawn and simulated in HFSS software which is shown in Fig. 5.5.

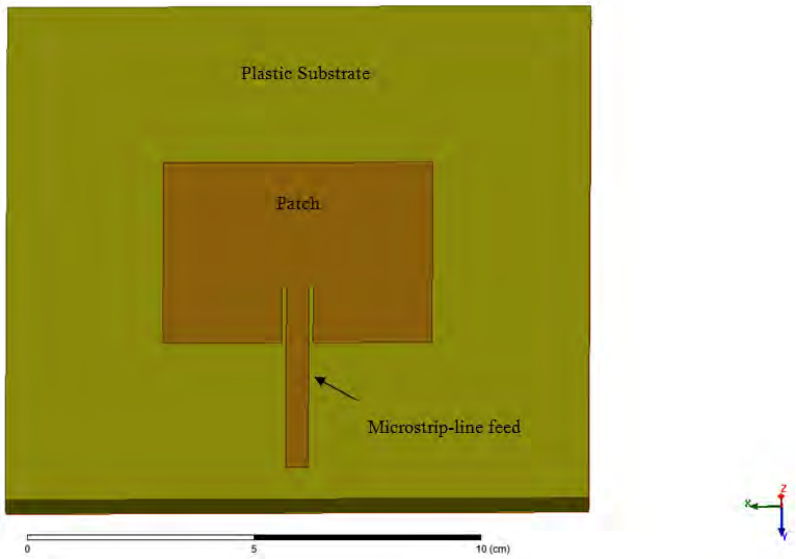

Fig. 5.5: GSM 1800 MHz patch antenna loaded with plastic substrate drawn in HFSS Software.

Frequency sweep was performed from 500 MHz to 3000 MHz. From the s-parameter of the antenna (Fig. 5.6), it is seen that good resonance occurs at 1.7 GHz, which is the first order mode of the antenna.

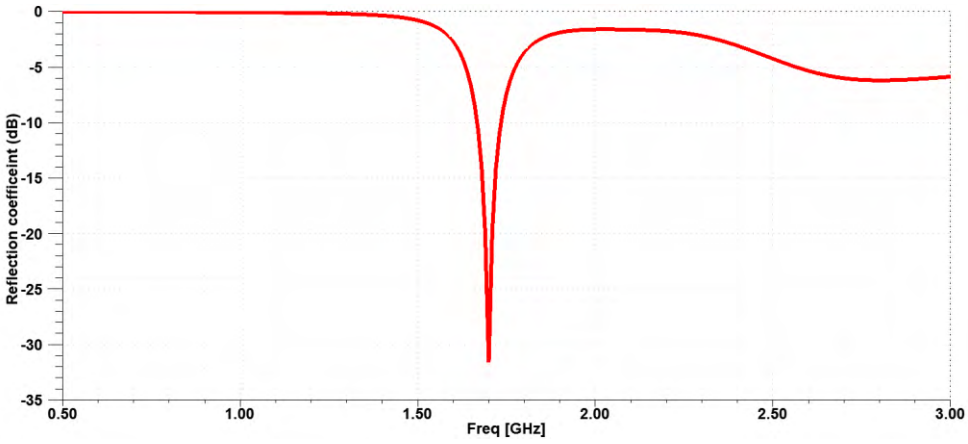

Fig. 5.6: S-parameter of the 1800 MHz patch antenna loaded with plastic substrate.

The radiation pattern of the antenna was investigated at its fundamental mode at 1.7 GHz. It is seen from Fig. 5.7 that the gain at the broadside is 7.01 dB. The sides lobes are also minor which is always desirable in antenna communication.

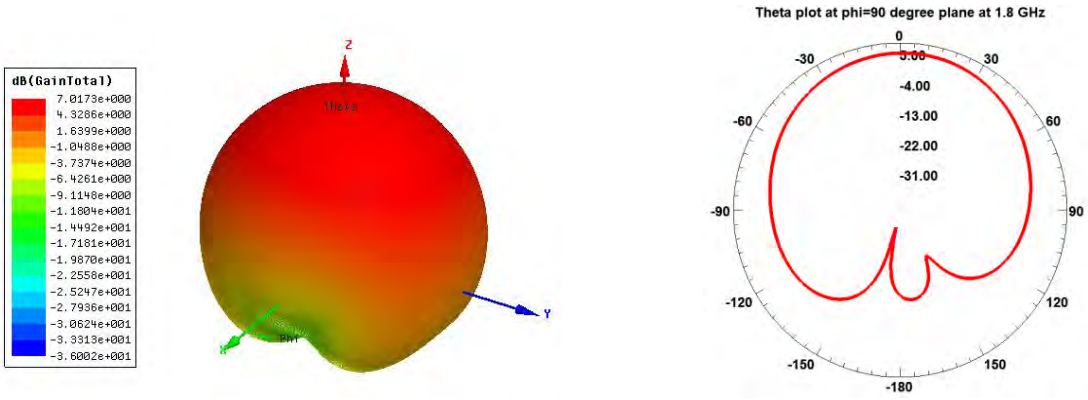

(a) (b)

Fig. 5.7: Radiation pattern of 1800 MHz plastic loaded patch antenna at 1.8 GHz, (a) 3-D radiation pattern (b) 2-D radiation pattern in theta plane at phi=90°.

5.2.3 GSM 1800 MHz Patch Antenna Loaded with Barium Titanate Substrate:

Using the same method as section 5.2.1 and 5.2.2, a very small rectangular patch antenna at GSM 1800 MHz frequency band was drawn and simulated in HFSS software as shown in Fig. 5.8. All the dimensions of the practically fabricated prototype was maintained , however, as a substrate, a hypothetical dielectric having a permittivity of 32.23 was modeled in HFSS since barium titanate material was not available its material directory. However, all the electric and chemical properties of barium titanate were kept similar in that hypothetical substrate.

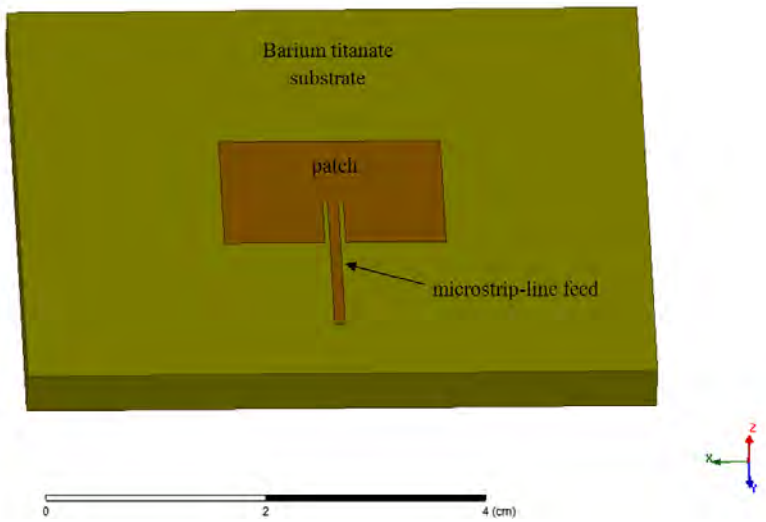

Fig. 5.8: GSM 1800 MHz patch antenna loaded with barium titanate substrate drawn in HFSS software.

Frequency sweep was performed from 0.5 GHz to 3 GHz to investigate the resonance properties. As seen from Fig. 5.9, there is a notch in s-parameter graph at frequency 1.8 GHz which is the fundamental mode of the antenna. It is observed that the value of reflection coefficient at the resonant frequency is about -6 dB. But for an antenna to operate efficiently, it is supposed to fall below -10 dB at the resonant frequency [50]. The reason for this may be due to using a very high permittivity material as the substrate. Moreover, the transmission line used for feeding the antenna was supposed to be 50 ohm for inset feed method. Since the width of the antenna was only around 20 mm, it was not possible to exactly cut the upper patch precisely for feeding it with a 50 ohm transmission line. In fact, the microstrip line width was kept at 1 mm instead of calculated 0.8 mm. All these factors might have contributed to impedance mismatch and consequently a lesser value of the return loss.

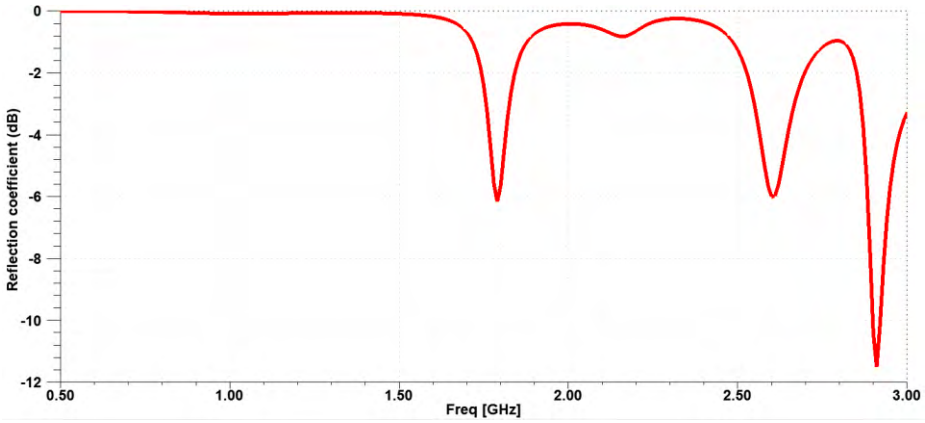

Fig. 5.9: S-parameter of the 1800 MHz patch antenna loaded with barium titanate substrate.

In Fig. 5.10, the gain of the patch antenna is investigated. It is seen that gain is also affected due to using a high permittivity material. The maximum total gain at the broadside is found to be 4.49 dB. It can be said that this sort of antenna is a trade off between smaller size and deteriorated gain performance.

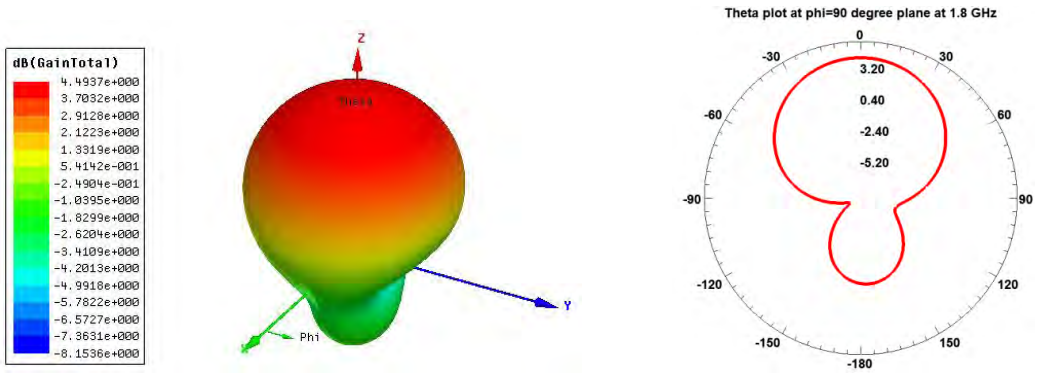

(a) (b)

Fig. 5.10: Radiation patterns of 1800 MHz barium titanate substrate loaded patch antenna at 1.8 GHz, (a) 3-D radiation pattern (b) 2-D radiation pattern in theta plane at phi=90°.

5.3 Comparison of Experimental and Simulation Results

The performances of all the fabricated antennas were compared with their simulation results, performed in HFSS and CST Microwave Studio software. The results obtained in HFSS are used here for comparison.

5.3.1 GSM 900 MHz Patch Antenna Loaded with Plastic Substrate

The GSM 900 MHz patch antenna loaded with plastic substrate were tested in laboratory and its radiation pattern in horizontal (phi) plane at theta=30° was observed which is shown in Fig. 5.11(a). In Fig. 5.11(b), the simulation result is shown.

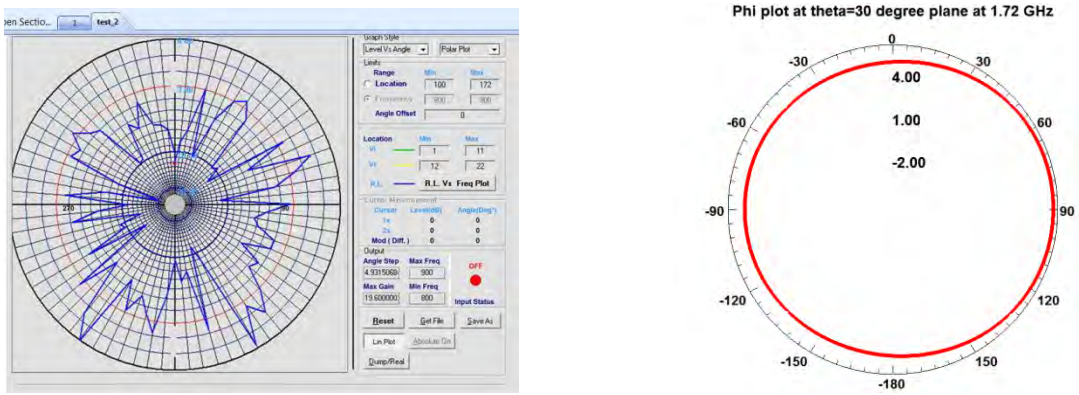

(a) (b)

Fig. 5.11: 2-D radiation pattern comparison in phi plane at 900 MHz (theta=30° cut) for 900 MHz plastic loaded patch antenna, (a) Experimental result (normalized signal strength in dB) (b) Simulation result.

From the above figure, it is evident that, although the simulation result of the patch antenna shows an omni-directional radiation pattern in the azimuth plane, the experimental result shows some fluctuations at different points. The cause for this might be non-ideal measurement environment in the laboratory as described in chapter 4.

5.3.2 GSM 1800 MHz Patch Antenna Loaded with Plastic Substrate:

The experimental and simulation radiation characteristics of the antenna were compared as shown in Fig. 5.12. It is seen that the pattern in theta plane is similar in both the cases. It was not possible to measure the gain of the patch in dB practically. Instead, signal strength was measured in dB unit. In Fig. 5.12(a), the maximum signal strength during measurement was found to be 7.11 dB at theta=0°. On the other hand, the maximum gain in simulation was found to be 7.01 dB at broadside. Therefore, the results seem to be concur each other.

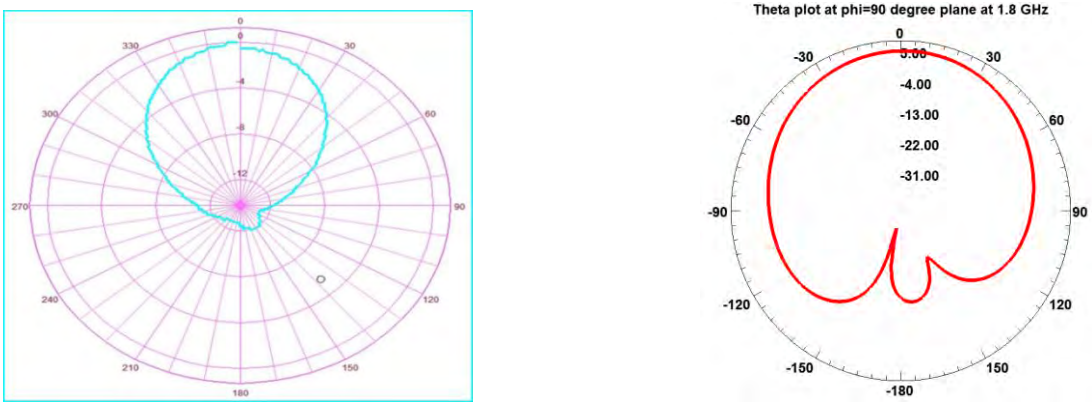

(a) (b)

Fig. 5.12: 2-D radiation pattern comparison in theta plane at 900 MHz (phi=90° cut) for 1800 MHz plastic loaded patch antenna, (a) Experimental result (normalized signal strength in dB) (b) Simulation result.

5.3.3 GSM 1800 MHz Patch Antenna Loaded with Barium Titanate Substrate:

Following the same procedure as in section 5.3.1, the experimental and simulation radiation characteristics of the antenna made of barium titanate substrate were compared as shown in Fig. 5.13. The 2-D radiation patterns of the antenna look quite similar. However, as shown in Fig. 5.13(a), the maximum signal strength of 3.97 dB is found at

theta=240° direction as opposed to broadside. This may be due to misalignment of the antenna during measurement in the laboratory. The cause of low gain may be attributed to the surface waves created due to the high permittivity material as substrate. Again from the simulation result in Fig. 5.13(b), it is seen that the maximum gain seen at broadside is 4.49 dB.

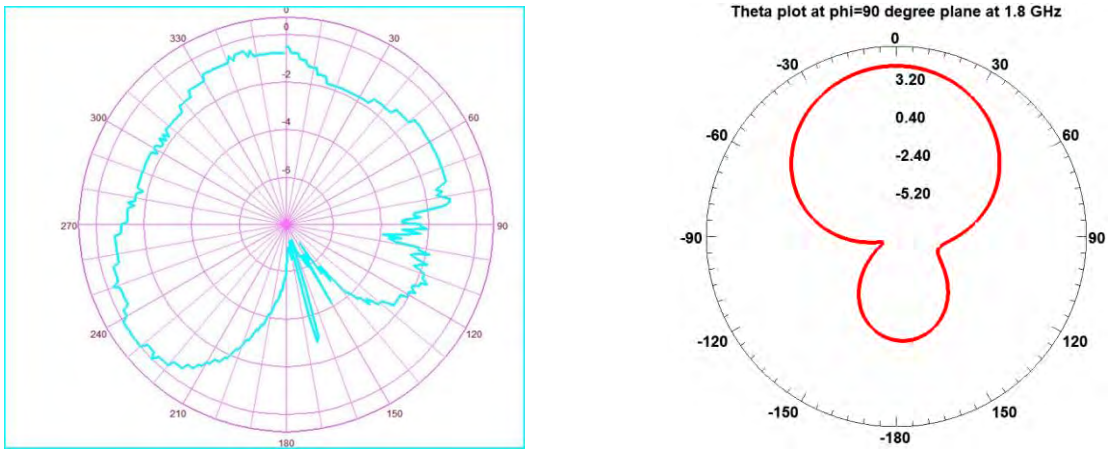

(a) (b)

Fig. 5.13: 2-D radiation pattern comparison in theta plane at 900 MHz (phi=90° cut) for 1800 MHz barium titanate loaded patch antenna, (a) Experimental result (normalized signal strength in dB) (b) Simulation result.

Chapter 6

Conclusion and Future Scope of Work

6.1 Conclusion of the Work

In this research, experimental investigation has been done for fabricated antennas at some desired frequency bands (GSM 900 MHz and 1800 MHz).Three patch antennas loaded with different substrates were fabricated and tested in the laboratory. The first fabricated antenna with plastic substrate at GSM 900 MHz did not show appreciable radiation characteristics. Instead of getting an omnidirectional radiation pattern in phi direction, irregular shaped pattern was obtained. The other two antennas loaded with both plastic and barium titanate substrate showed good radiation characteristics at 1800 MHz. It is mentionable that size reduction was the only factor considered in fabricating a patch antenna with a high permittivity material like- barium titanate. It is found from simulations that all the antennas show quite good similarity with its experimental results.

In most of the cases, the experimental results seem to show a lesser gain than the simulations. This is because of the fact that in simulation always ideal environment is considered, which is not the case for experimentation with the fabricated antennas in laboratory. Surface waves, impurity in the substrates, non-anechoic chamber in the laboratory etc. are the factors for which the performance of the fabricated antennas deviate from ideal cases. Due to limitations of fabrication materials and laboratory equipments, it was not possible to fabricate more complicated antenna structure and test them. The main challenge in designing these sort of patch antennas is determining the permittivity of the substrate, on the basis of which later other parameters are fixed. Although impedance analyzer has been used to determine the permittivity from its capacitance at different frequencies, this method is not beyond error. The length and

width of the antennas were properly fixed according to the permittivity of material, but a slight deviation in these parameters might have caused shift in their resonant frequencies and radiation patterns as evident from the experimental results. On top of that, s-parameter is a very important parameter in any antenna design, which was not possible to measure, as network analyzer required for this sort of measurement was not available in the laboratory. Despite all these shortcomings, all three fabricated antennas work reasonably well in the desired frequency bands.

6.2 Scope for Future Work

Although it was not possible to observe all sorts of experimental results of the fabricated antennas due to the limitation of lab equipments, the simulation results of these antennas agree well with the experimental data and results as described in chapter 5. However, the followings can be done to improve the performance of these sorts of patch antennas-

- If the second order mode of 900MHz antenna is modified by cutting symmetric slots over the patch, we can have dual band performance from a single antenna which may cover both 900MHz and 1800 MHz frequencies. Due to cutting symmetric slot, the radiation at both the bands will be broad-sided. The same thing can be done for 1800 MHz patch antennas to cover 1800 MHz and 3600 MHz band.
- The bulky substrate material may be replaced with a material of high permittivity. Although it will cause less radiation efficiency, still it may reduce the antenna size and weight. The experimental investigation of the patch antenna loaded with artificial barium titanate substrate has been given. However, the laboratory manufacturing of barium titanate is a cumbersome process which urges the necessity for some easily manufacturable less bulky and high permittivity material.

References

[1] Balanis, C. A. "Antenna Theory: Analysis and Design," Third Edition, *John Wiley and Sons, 2005.*

[2] James, J. R. "Handbook of Microstrip Antennas," *Peter Peregrinus Ltd. : London*, 1989.

[3] Pozar, D. M., and Schaubert, D. H. "Microstrip antennas: The analysis and design of microstrip antennas and array,*." IEEE Press, Piscataway, NJ*, 1995.

[4] Wong, K. L. "Compact and Broadband Microstrip Antennas," *Wiley,* 2002.

[5] Kumar, G., and Ray, K. P. "Broadband Microstrip Antennas," *Artech House, Boston*, 2003.

[6] Ferdous, S.*,* Hossain, A., Chowdhury, S. M. H., Mahdy, M. R. C.*,* and Matin, M. A. "Reduced and Conventional sized Multi-Band Circular Patch Antennas Loaded with Metamaterials," *IET Microwaves, Antennas and Propagation* , vol. 7, pp. 768-776, 2013.

[7] Hossain, M. A., Ferdous*,* S., Chowdhury, S. M. H. and Matin, M. A. "Novel Dual Band Microstrip Circular Patch Antenna Loaded with MNG and ENG metamaterials," *International Journal of Antennas and Propagation*, vol. 2014, http://dx.doi.org/10.1155/2014/904374.

[8] Prasad, T. Durga, Kumar, K. V. Satya, Muinuddin, MD Khwaja Chisti , Kanthamma, B., and Kumar, V. Santosh "Comparisons of Circular and Rectangular Microstrip Patch Antennas." *International Journal of Communication Engineering Applications*, vol. 02, issue. 04, 2011.

[9] Jahani, S., Rashed, M. J., and Shahabadi, M. "Miniaturization of Circular Patch Antennas Using MNG Metamaterials," *IEEE Antennas and Wireless Propagation Letters*, vol. 9, pp. 1194-1196, 2010.

[10] Islam, F., Ali, M., Majlis, B.Y., and Misran, N."Design, simulation and fabrication of microstrip patch antenna for dual band application," *International Conference on* Electrical and Computer Engineering, pp. 799-802, 2008.

[11] Bordoloi, A. K., Borah, P., Bhattacharyya, S., Bhattacharyya, N. S. "A novel approach for post fabrication fine tuning and matching of microstrip patch antenna using adjustable air pocket in substrate layer," *Antennas and Propagation Conference (LAPC),* pp. 1-3, 2011.

[12] Dey, D., and Kshetrimayum, R. S. "High Gain and Efficient Patch Antenna on Micromachined GaAs EBGs with Increased Bandwidth," *Annual IEEE India Conference*, pp. 1-5, 2006.

[13] Wee, F.H., Malek, F., Al-Amani, A. U., and Ghani, F. "Effect of Two Different Superstrate Layers On Bismuth Titanate (BiT) Array Antennas," *Scientific Reports 4*, Article number: 3709, 2014. doi:10.1038/srep03709.

[14] Wong, K. L., and Hsieh, K. B. "Dual-frequency circular microstrip antenna with a pair of arc-shaped slots," *Microwave Opt. Technol. Lett.* 19, 410–412, 1998.

[15] Hsieh, K. B., and Wong, K. L. "Inset-microstrip-line-fed dual-frequency circular microstrip antenna and its application to a two-element dual-frequency microstrip array*," IEE Proc. Micro Antennas Propagat.* 147, 359–361, 1999.

[16] Jan, J.Y., and Wong, K. L. "Single-feed dual-frequency circular microstrip antenna with an open-ring slot," *Microwave Opt. Technol. Lett*. 22, 157–160, 1999.

[17] Heinrich Hertz: *The Discovery of Radio Waves*, http://www.juliantrubin.com.

[18] Antenna-theory website, http://www.antenna-theory.com/basics/bandwidth.php.

[19] Antenna polarization, http://www.air-stream.org.au/technical-references/antenna-polarisation.

[20] Antenna Magnus 2015, http://www.antennamagus.com.

[21] Carver, K. R., and Mink, J. W. "Microstrip Antenna Technology," *IEEE Trans. Antennas Propagat.*, vol. AP-29, no. 1, pp. 2-24, 1981.

[22] Lo, Y. T., Soloman, D., and Richards, W. F. “Theory and Experiments on Microstrip Antennas,” *IEEE Trans. Antennas Propagat.*, vol. AP-27, no. 2, pp. 137-145, 1979.

[23] Richards, W. F., Lo, Y. T., and Harrison, D. D. “ An Improved Theory of Microstrip Antennas with Applications,” *IEEE Trans. Antennas Propagat.,* vol. AP-29, No. 1, pp. 38-46, 1981.

[24] Bailey, M. C., and Deshpande, M. D. “Integral Equation Formulation of MIcrostrip Antennas,” *IEEE Trans. Antennas Propagat.,* vol. AP-30, No. 4, pp. 651-656, 1982.

[25] Bahl, I. J., and Bhartia, P. “ Microstrip Antennas,” *Artech House,* Dedham, MA, 1980.

[26] Katehi, P. B., and Alexopoulos, N. G. “ On the Modeling of Electromagnetically Coupled Micrstrip Antennas- The Printed Strip Dipole,” *IEEE Trans. Antennas Propagat.,* vol. AP-32, No. 11, pp. 1179-1186, 1984.

[27] Oltman, H. G., and Huebner, D. A. “ Electromagnetically Coupled Micostrip Dipoles, ” *IEEE Trans. Antennas Propagat.*, vol. AP-29, No. 1, pp. 151-157, 1981.

[28] Pozar, D. M. “A Microstrip Antenna Aperture Coupled to a Microstrip Line,” *Electronic Letters*, vol. 21, pp. 49-50, 1985.

[29] Gronau, G., and Wolff, I. “Aperture-Coupling of a Rectangular Microstrip Resonator,” *Electronic Letters*, vol. 22, pp. 554-556, 1986.

[30] Bahl, I. J. and Trivedi, D. K. "A Designer Guide to Microstrip Line," *Microwaves,* p. 174, 1977.

[31] Kumar, A., and Sharma, S. “Measurement of Dielectric Constant and Loss Factor of the Dielectric Material at Microwave Frequencies,” *Progress In Electromagnetics Research, PIER* 69, pp. 47–54, 2007.

[32] Krupka, J. “Frequency domain complex permittivity measurements at microwave frequencies,” *Institute of Physics Publishing Meas. Sci. Technol.* 17 (2006) R55–R70 doi:10.1088/0957-0233/17/6/R01.

[33] MATLAB and Statistics Toolbox Release 2012b, The MathWorks, Inc., Natick, Massachusetts, United States.

[34] Frost, N. E., and McGrath, P. B. "Dielectric properties of barium titanate and alumina filled epoxy," *Conference on Electrical Insulation and Dielectric Phenomena,* pp. 564-567, 1995.

[35] Schaubert, D. H., Pozar, D. M., Adrian, A., "Effect of microstrip antenna substrate thickness and permittivity: comparison of theories with experiment," *IEEE Transaction on Antennas and Propagation,* vol.37, pp. 677-682, 1989.

[36] Manteghi, M., "Wideband microstrip patch antenna on a thick substrate," *Antennas and Propagation Society International Symposium*, pp. 1-4, 2008.

[37] Chand, S., A. Sathyanarayanan, and Khan, A. U. "Antenna calibration in anechoic chamber," *9th International Conference on Electromagnetic Interference and Compatibility (INCEMIC),* pp. 541-544, 2006.

[38] Zhang, H.S., Chai, S. L., Xiao, K. and Ye, L. "Numerical and Experimental Analysis of Wideband E-shaped Patch Textile Antenna," *Progress in Electromagnetics Research*, vol. 45, pp. 163-178, 2013.

[39] Hang, W., Luk, K. M. , Chan, C. H., Xue, Q., So, K. K. and Lai, H.W. "Small Antennas in Wireless Communications," *IEEE Transaction on Antennas and Propagation,* vol. 100, pp. 2109-2121, 2012.

[40] Ertuğ, Burcu. "The Overview of The Electrical Properties of Barium Titanate," *American Journal of Engineering Research (AJER),*vol. 02, iss. 08, pp-01-07, *2013.*

[41] Hoop, A.T., and Jong, G.D. "Power Reciprocity in Antenna Theory," *IEE Proceedings* , vol. 121, iss. 10, pp. 1051-1056, 1974.

[42] Kumar, A. "Gain and Directivity Analysis of the Log Periodic Antenna," *International Journal of Scientific Engineering and Research*, vol.1, iss. 3, 2013.

[43] Rumsey, V. H. "Frequency Independent Antennas," *IRE national convention record*, Part I, pp. 114-118, 1957.

[44] 4nec2 Antenna Modeler and Optimizer, available at: http://www.qsl.net/4nec2/.

[45] Antenna Training System-Scientech 2261, available at: scientechworld.com.

[46] Herscovici, N., Cipus, Z., and Kildal, P. S. " The cylindrical omnidirectional patch antenna," *IEEE Transaction of Antennas and Propagation,* vol. 49, pp. 1746 – 1753, 2001.

[47] Li, K., Cheng, Matsui, C. H. T., and Izutsu, M. "Simulation and experimental study on coplanar patch and array antennas," *Asia-Pacific Microwave Conference*, Dec. 2000. doi: 10.1109/APMC.2000.926100.

[48] ANSYS HFSS, version 13.0, build: July 18, 2007, Ansoft Corporation, http://www.ansoft.com.

[49] CST Microwave Studio 2009, CST of America [Online]. Available: http://www.cst.com.

[50] Okhowat, M., Fallahi, R., "Measurements of Antenna Reflection Coefficients in Time Domain," *International Conference on Mathematical Methods in Electromagnetic Theory,* pp. 328-330, 2006.